Abstract Book

4th Emallia Conference

Hokkaido Univ.-Pusan Univ.-RIKEN Symposium

Hokkaido University,
23th-25th of July, 2018

(1) Oral Presentations
(2) Poster Presentations

(1) Oral Presentations

23th of July
@Academic rounge 1 & 2 in the faculty of engineering (9:40-18:45)

24th of July
@Academic rounge 1 & 2 in the faculty of engineering (9:00-18:00)

25th of July
@2-211 in the faculty of science (9:30-15:00)

High-T_c mechanism of iron-based superconductors

Hiroyuki Yamase[1,2] and Tomoaki Agatsuma[1,2]

[1] *National Institute for Materials Science, Tsukuba, Japan*
[2] *Graduate School of Science, Hokkaido University, Sapporo, Japan*

Iron-based superconductors were discovered as a new family of high-T_c superconductivity [1]. Typically the superconducting phase is realized close to the spin-density-wave phase and spin fluctuations are believed to be an important source to drive superconductivity. A close look at the phase diagram reveals that the superconducting phase is closer to the so-called electronic nematic phase where the fourfold symmetry is broken spontaneously by electronic correlations. Hence fluctuations associated with the nematic phase are also expected to play an important role for superconductivity.

In this talk, we consider nematic fluctuations originating from the occupation difference of d_{xz} and d_{yz} orbitals, namely *orbital nematic fluctuations* and show that the orbital nematic fluctuations can be a new high-T_c mechanism of iron-based superconductors. We study a minimal two-band model consisting of d_{xz} and d_{yz} orbitals, where electrons interact with each other via orbital nematic and spin-exchange interactions. We then compute the onset temperature of superconductivity as well as the momentum dependence of the paring gap by including the electronic self-energy effect in the framework of the Eliashberg theory. Technically there are two successes: inclusion of the self-energy effect and computation at low temperature which allows us to evaluate T_c of superconductivity. We find that (i) orbital nematic fluctuations can drive superconductivity with T_c comparable with experimental data [2, 3], (ii) spin fluctuations, on the other hand, are less effective for the superconducting instability, although they can drive superconductivity [4], and (iii) orbital nematic and spin fluctuations work competitively for the superconducting instability and high-T_c is achieved when orbital nematic fluctuations are dominant [4].

[1] Y. Kamihara, T. Watanabe, M. Hirano, and H. Hosono, J. Am. Chem. Soc. **130**, 3296 (2008).
[2] H. Yamase and R. Zeyher, Phys. Rev. B **88**, 180502(R) (2013).
[3] T. Agatsuma and H. Yamase, Phys. Rev. B **94**, 214505 (2016).
[4] T. Agatsuma, Ph. D. thesis, Hokkaido University.

2018. 07. Emillia conference (due on 9 July)

Investigation the origin of charge carrier in NiO by Na doping

Seojin Yang[1], Jiwoong Kim[1], Jong-Seong Bae[2], Sungkyun Park[1,*]

[1]*Department of Physics, Pusan National University, Busan 46241, Korea*

[2]*Busan Center, Korea Basic Science Institute, Busan 46742, Korea*

Transparent conductive materials have been consistently attracted due to demand of advanced transparent electrodes. NiO which has large band-gap of 3.6 ~ 4.0 eV, chemical stability and *p*-type characteristic is one of the good candidates as advanced transparent electrode materials. However, due to the lack of hole concentration, it is not easy to be used in current application. Therefore, improving hole carrier concentration, understanding the source of the conducting charge, and mechanism are important subjects of recent research field. In this study, we demonstrated the possible controlling electrical properties by Na-doping on NiO powders. Electrical resistivity of Na-doped NiO was increased with increasing Na doping (until 9%) even though it possesses *n*-type characteristics, except for the sample under 1% doping. Interestingly, the portion of oxygen vacancy was enhanced with Na contents examined by X-ray photoelectron spectroscopy. This suggest that oxygen vacancy is able to act as donor in NiO system.

This study was supported in part by NRF Korea (NRF-2017K1A3A7A09016305 and NRF-2018R1D1A1B07045663).

[*]E-mail: psk@pusan.ac.kr

ESR study of the triangular lattice system X[Pd(dmit)$_2$]$_2$

Sunghyun Kim[1,2], Yugo Oshima[1,2], Reizo Kato[2]

***Hokkaido Univ.*[1], *RIKEN*[2]**

The magnetic ground state of S=1/2 antiferromagnetic triangular lattice has been debated for many decades in condensed matter physics since the ground state is highly degenerated due to the geometrical frustration of the spins, and the anion radical salt X[Pd(dmit)$_2$]$_2$ (X is a monovalent cation) is one of the materials which consists of S=1/2 antiferromagnetic triangular lattice. A wide variety of ground states, such as quantum spin-liquid (QSL) state, antiferromagnetic long-range ordered (AFLO) state, charge-ordered (CO) state have been observed depending on the degree of geometrical frustration (frustration parameter t'/t) controlled by the monovalent cation X (Fig. 1). Especially, EtMe$_3$Sb[Pd(dmit)$_2$]$_2$ does not exhibit long-range order down to 30 mK, and spin-liquid like behavior is observed in the heat capacity and NMR measurements [1]. However, the nature of the QSL state, whether the excited state is gapless or gapped, is not clarified yet. For example, heat capacity, thermal conductivity suggest a gapless excitation, whereas NMR measurement suggests a gapped excited state.

We have previously reported that unconventional behaviors of the ESR linewidth are observed by ESR measurement [2]. We propose that the ESR is directly observing the spinon, which is the elementary excitation of QSL state, and the peculiar ESR linewidth behavior reflects the dynamics of the spinon. However, it is still not clear how much spin is contributing to the spin excitation. Therefore, we have verified the spin density of the X[Pd(dmit)$_2$]$_2$ system by using the spin counting method of ESR. In the presentation, we present our results of the spin counting for several X[Pd(dmit)$_2$]$_2$ salts, and its ground state is discussed.

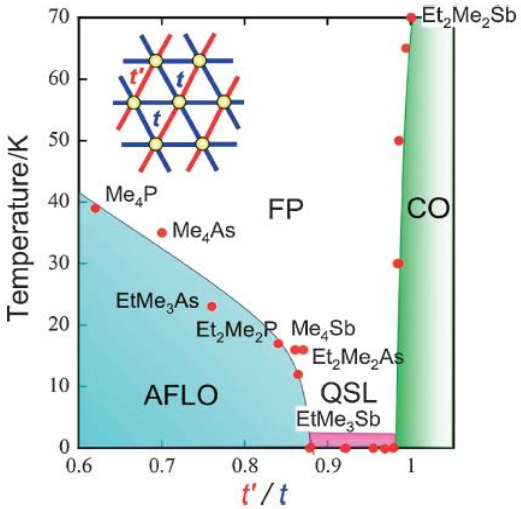

Fig. 1 Phase diagram of X[Pd(dmit)$_2$]$_2$ [1]

Reference

[1] R. Kato, Bull. Chem. Soc. Jpn., 87 (2014) 355-374.

[2] 大島勇吾 他, 日本物理学会, 第 70 回年次大会, 24pAB-11

Nonreciprocal magnon excitations on a breathing kagome lattice

[1]T. Matsumoto, [1]S. Hayami
[1]*Dept.of Phys., Hokkaido Univ.*

In condensed matter physics, the breakings of time-reversal and spatial inversion symmetries give rise to fascinating phenomena, such as magneto-optical and magneto-electric effects. Among them, nonreciprocal phenomena, which shows a rectification, have been much interest, since they induce unconventional transport properties and excitations. From a microscopic point of view, nonreciprocal phenomena in metallic systems occur once the wave numbers of electrons $\boldsymbol{k}$ and $-\boldsymbol{k}$ are inequivalent in the absence of both time-reversal and spatial inversion symmetries. Meanwhile, besides metals, similar nonreciprocal physics also occurs even in noncentrosymmetric magnetic insulators. There, magnon excitations show a rectification, which originates from the interplay between the Dzyaloshinskii-Moriya (DM) and exchange interactions [1–4]. Recently, such nonreciprocal magnon excitations were observed in a noncentrosymmetric ferromagnet $LiFe_5O_8$ through microwave absorption spectra [1] and α-$Cu_2V_2O_7$ by inelastic neutron scattering experiment [2]. Moreover, interesting possibilities of further nonreciprocal physics, such as the nonreciprocal optical effect [5, 6] and nonreciprocal spin Seebeck effect [3, 4], have been extensively studied. However, the conditions to obtain nonreciprocal magnon excitations have not been fully understood. It is desirable to clarify fundamental ingredients to obtain such nonreciprocal magnon excitations.

Motivated by these studies, we investigate when and how nonreciprocal magnon excitations are realized in magnetic insulators. We here consider a breathing kagome system in the absence of spatial inversion symmetry. First, we construct a spin model with symmetric anisotropic exchange and antisymmetric DM interactions in addition to the isotropic one from the symmetry point of view. Next, we calculate the ground-state phase diagram of the model in a wide range of model parameters. By examining magnon excitations for each magnetic ordering within the Holstein-Primakoff approximation, we clarify the conditions to obtain nonreciprocal magnon excitations from the symmetry point of view. Furthermore, we find the toroidal moments degree of freedom, which are often accompanied with magnetic orderings in noncentrosymmetric crystals, play an essential role in realizing nonreciprocity. In the presentation, we discuss what types of nonreciprocal magnon excitations are realized in various type of magnetic orderings and clarify a role of toroidal moments microscopically.

[1] Y. Iguchi, S. Uemura, K. Ueno, and Y. Onose, Phys. Rev. B **92**, 184419 (2015).

[2] G. Gitgeatpong *et al.*, Phys. Rev. Lett. **119**, 047201 (2017).

[3] R. Takashima, Y. Shiomi, and Y. Motome, Phys. Rev. B **98**, 020401(R) (2018).

[4] Y. Shiomi *et al*, Phys. Rev. B **96**, 180414(R) (2017)

[5] Y. Takahashi *et al*, Nature Physics **8**, 121 (2012)

[6] S. Miyahara and N. Furukawa, J. Phys. Soc. Jpn. **81**, 023712 (2012); Phys. Rev. B **89**, 195145 (2014).

Combined DFT and STM studies of SnSe and $SnSe_{1-x}S_x$ alloys

Taewon Min[1], Ganbat Duvjir[2], Trinh Thi Ly[2], Jinho Byun[1], Taehoon Kim[2], Mahmoud M. Saad[2], Nguyen Thi Minh Hai[2], Anh-Tuan Duong[2], Sunglae Cho[2], S.H. Rhim[2], Jungdae Kim[2], Jaekwang Lee*[1]

[1]*Pusan National University, Department of Physics, Busan 46241, South Korea*
[2]*Ulsan University, Department of Physics, Ulsan 44610, South Korea*

E-mail: jaekwangl@pusan.ac.kr

SnSe single crystal has been found to exhibit excellent thermoelectric performance with an extremely high ZT (figure of merit) value of 2.6. Although this high ZT value has attracted considerable attention, the origin of p-type character of SnSe has yet to be clearly understood. Here, by combining scanning tunneling microscopy (STM) and density functional theory (DFT) calculations, we find that the most dominant Sn vacancies generate the defect state inside the dispersive valence band and produce extra holes throughout the entire system. On the other hand, other intrinsic vacancies create a nondispersive donor level and generate immobile electrons localized near the vacancy site. Our combined STM/DFT studies can provide important information for the development of highly efficient SnSe-based thermoelectric devices. In addition, we will show the structural evolution of $SnSe_{1-x}S_x$ alloys at the atomic level.

This work was supported by the National Research Foundation of Korea (NRF) grant funded by the Korea government (2018R1A2B6004394). Also this work was supported by the National Research Foundation of Korea (NRF) Grant funded by the Korean government (MSIP) (NRF-2015R1C1A1A01053810).

First-principles studies of complex oxides interfaces

Taewon Min, Jinho Byun and Jaekwang Lee*

[1]*Department of Physics, Pusan National University, Busan 46241, South Korea*

Corresponding author. E-mail: Jaekwangl@pusan.ac.kr

Abstract

The Oxide interfaces have attracted considerable attention in recent years due to emerging novel properties that do not exist in the corresponding parent compounds. Furthermore, modern atomic-scale growth and probe techniques enable the formation and study of new artificial interface states distinct from the bulk state. A central issue in understanding the novel phenomena in oxide heterostructures is to reveal how various physical variables (spin, charge, lattice and/or orbital hybridization) interact with each other. Here, using density functional theory calculations, we explore the electronic, magnetic and structural properties developed near the complex oxide interfaces such as $SrTiO_3/LaAlO_3$ and $Fe/PbTiO_3$. We study the interplay between physical interactions, and quantify parameters that determine physical properties of heterostructures. Our theoretical studies help understanding how physical variables couple with each other and how they determine new properties at oxide interfaces.

Multi-frequency ESR studies of the π-d molecular conductor λ-$(STF)_2FeCl_4$

Taehoon Lee[1,2], Yugo Oshima[1,2], Takaaki Minamidate[1], Yohei Saito[2], Atsushi Kawamoto[2], Noriaki Matsunaga[2] and Reizo Kato[1]

RIKEN[1], Hokkaido University[2]

λ-$(BETS)_2FeCl_4$ is a π-d molecular conductor with strong π-d interaction. Due to this π-d interaction, this system has a fascinating phase diagram [1]. We have previously investigated λ-$(BETS)_2FeCl_4$ using ESR spectroscopy. Typical angular dependence of the g-value has a sinusoidal curve, however, anomalous minima of the g-value was observed [2]. We think the origin of the minima is due to the π-d interaction between Se or S in the BETS molecule and $FeCl_4^-$ anion. For understanding the π-d interaction effect, we have investigated another π-d system, which is λ-$(STF)_2FeCl_4$. λ-$(STF)_2FeCl_4$ is an insulator and becomes a conductor under pressure, and antiferromagnetic long-range order is observed below T_N=16 K [3]. STF is an asymmetric molecule, half side is the same with BETS and the other half has no Se atoms as shown Fig. 1. Hence, similar π-d interaction with λ-$(BETS)_2FeCl_4$ is expected for the half BETS side, but, the other half has only contact with S atoms.

In the previous theoretical study, the easy-axis of λ-$(BETS)_2FeCl_4$ is tilted 30° from the c-axis due to the π-d network [4]. The antiferromagnetic resonance of λ-$(STF)_2FeCl_4$ is observed when the magnetic field is tilted 35° from the c-axis. It suggests the easy-axis of λ-$(STF)_2FeCl_4$ is also tilted from the c-axis. Hence, the π-d interaction in λ-$(STF)_2FeCl_4$ seems to exist. However, λ-$(STF)_2FeCl_4$ has the typical angular dependence of the g-value in contrast with λ-$(BETS)_2FeCl_4$ as shown Fig. 2. Hence, the π-d interaction of λ-$(STF)_2FeCl_4$ might be weaker than λ-$(BETS)_2FeCl_4$.

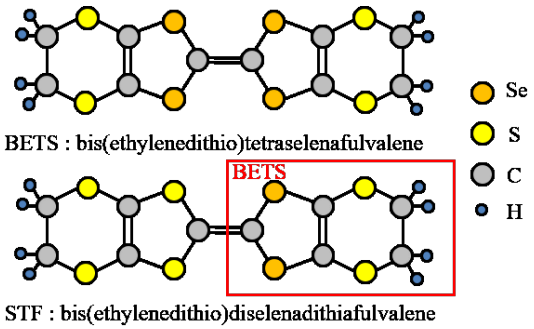

Fig. 1. Structure of BETS and STF molecules

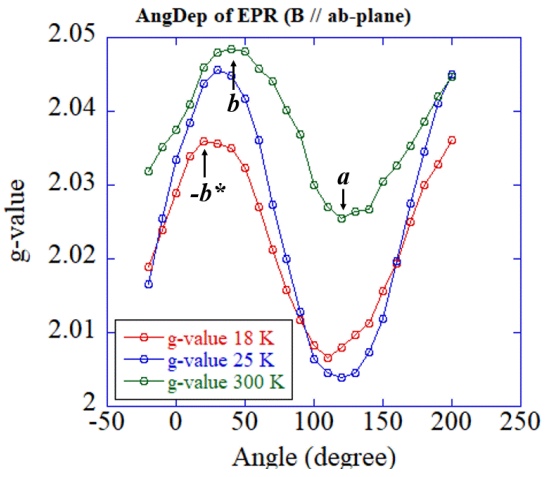

Fig. 2. Angular dependence of the g-value of λ-$(STF)_2FeCl_4$

Reference
[1] Y. Oshima *et al*., Magnetochemistry, 3(1) (2017) 10
[2] T. H. Lee *et al*., 72nd Annual JPS meeting, 17aC21-4, March 17-20 2017
[3] T. Minamidate *et al*., Phys. Rev. B **97** (2018) 104404
[4] H. Shimahara *et al*., J. Phys. Soc. Jpn. **85** (2016) 043708

Many-Body Effects in Bose-Einstein Condensates(BECs)

Dept. of Phys., Hokkaido Univ.
A. Kirikoshi

Bose-Einstein condensation is a phase transition phenomenon in which macroscopic number of particles form a coherent state at a certain temperature in a multiparticle system. BEC has been studied actively in both experimental and theoretical approach.

Bogoliubov theory is a widely known as a theory describing a weakly interacting bosons[1]. According to this theory, an elementary excitation called Bogoliubov mode has a linear dispersion and an infinite lifetime in the long wavelength limit. However, Bogoliubov theory does not incorporate 3/2-body correlation, which is a particle exchange process between condensate and non condensate, and 2-body correlation, which is a process of momentum exchange between non-condensed particles. Costructing the self-consistent mean-field theory (Hartree-Fock-Bogoliubov (HFB) theory)[2] with the Bogoliubov mode as a thermal excitation, a finite energy gap appears in the one-particle excitation, which contradicts Hugenholtz-Pines theorem that the one-particle excitation must be a gapless excitation[3].

Recently, a variational wave function for the ground state of weakly interacting bosons incorportating the dynamical 3/2-body processes was constructed[4]. This wave function gives a lower energy than the HFB theory[2]. These processes are also shown (i) to transform the one-particle excitation into a bubbling mode having the finite lifetime even in the long wavelength limit and (ii) to correct the stability condition for 2-component miscible state[5].

To investigate the properties of many-body effects, we try to extend the variational approach to finite temperatures. First, we construct a variational density matrix incorporating 3/2-body correlations, and then evaluate the grand potential using Green's function. This method makes it possible to investigate the temperature dependence of the many-body effects in the BEC phase. We apply this method to a low temperatrue system and find that the 3/2-body correlations contribute to lowering the free energy as in the case of zero temperature system.

[1] N. N. Bogoliubov, J. Phys. (USSR) **11**, 23 (1947).

[2] M. Girardeau and R. Arnowitt, Phys. Rev. **113**, 755 (1959).

[3] N. M. Hugenholtz and D. S. Pines, Phys. Rev. **116**, 489 (1959).

[4] T. Kita, J. Phys. Soc. Jpn. **86**, 044003 (2017).

[5] W. Kohno, A. Kirikoshi, and T. Kita, J. Phys. Soc. Jpn. **87**, 034002 (2018).

Standard Model and Grand Unified Theory

Hikaru Uchida
Division of physics, Graduate School of Science, Hokkaido University

The interactions needed to compose atoms are electromagnetic (EM) interaction, weak interaction, and strong interaction. Natural phenomena can be explained by these three interactions other than gravity, and these are induced from the corresponding symmetries. In particular, EM interaction is induced from $U(1)_Q$ local symmetry depending on the EM charge the particle has. Weak interaction is induced from $SU(2)_L$ local symmetry between left handed up quark and down quark or neutrino and electron. And strong interaction is induced from $SU(3)_C$ local symmetry among three color charges that quarks have. However, since weak bosons, inducing weak interaction, have their mass, strictly there is no $SU(2)_L$ local symmetry. And weak bosons also have their EM charges. Then weak interaction and EM interaction, at higher energy scale, are originally the same interaction called electroweak interaction induced from $SU(2)_L \times U(1)_Y$ local symmetry. This symmetry is spontaneously broken at about 100GeV so weak interaction is induced by weak bosons which obtained their mass. On the other hand, EM interaction is induced from unbroken $U(1)_Q$ symmetry. Thus adding $SU(3)_C$ local symmetry inducing strong interaction to electroweak interaction, natural phenomena can be explained by $SU(2)_L \times U(1)_Y \times SU(3)_C$ local gage symmetry, which induces EM, weak, and strong interactions, other than gravity. This is the standard model.

However, there are the following mysteries in the standard model: (i) left-right asymmetry, (ii) strong interaction is independent of the other two interactions and quark-lepton asymmetry, and (iii) Abelian $U(1)_Y$ has some disadvantage such as unclear derivation of Y.

There is a model to overcome these mysteries. That model is the model with $SU(2)_L \times SU(2)_R \times SU(4)_C$ fundamental local gauge symmetry where fourth color is lepton number at the higher energy scale than that of the standard model. So this model, called the Patti-Salam Model, is a non-Abelian grand unified model for three interactions, those are EM, weak, and strong interactions with left-right and quark-lepton symmetry. In this model, there are two steps of spontaneous symmetry breaking: $SU(2)_L \times SU(2)_R \times SU(4)_C \rightarrow SU(2)_L \times U(1)_Y \times SU(3)_C \rightarrow U(1)_Q \times SU(3)_C$. Besides, I will show another approach to construct this model from string theory.

Reference

J. C. Pati, (2017) arXiv:1706.09531v1 [hep-ph]

The Standard Model from Superstring Theory

Yuki Kariyazono
Division of physics, Hokkaido University

Physics has developed with an idea of unification. Electricity and magnetism were united in 19th century, and electromagnetic force and weak force were united in 20th century. The electroweak theory together with QCD form the Standard Model. Now we can describe almost all experimental results using the Standard Model and the theory of relativity. However, there are many problems. For example, the Standard Model cannot describe quantum gravity. In the processes at short distance, non-renormalizable ultraviolet divergence appears. Many physicists believe that there is a unified theory of all forces in nature. The superstring theory is a candidate for a unified theory that reconcile the quantum theory and the theory of relativity. In superstring theory we introduce an extended object called a string with a minimal length. There are two types of string, an open string and a closed string. When we pay attention to open strings' boundary conditions, we can find that endpoints of all open strings are attached to some physical objects called D-branes. From the states of string attached to D-branes, we can obtain the same states as in the Standard Model.

Contribution to the power spectrum from curvature and radiation during pre-inflation era

Tadashi Sasaki and Hisao Suzuki
Department of Physics, Hokkaido University, Sapporo 060-0810, Japan

Inflation is exponential expansion of the universe which is now believed to have occured in the very early stage of our universe. This scenario can explain the flat power spectrum of the observed fluctuations in the cosmic microwave background (CMB), and resolve the flatness and horizon problem as well.

In this study, we consider the effect of spatial curvature, radiation, and inflaton potential energy, which are expected to dominate the pre-inflation era, on the power spectrum. Under the assumption that the energy scale of the inflation is much less than the Planck scale, at which quantum gravitational effect is no longer negligible, we can treat the spacetime geometry in classical general relativity, where time evolution of the universe is described by the Friedmann equation. First, we show that the Friedmann equation can be solved exactly by using the Weierstrass's elliptic functions $\wp(z)$. After that we consider a massless scalar field on that spacetime. The equation of motion turns out to be the Lamé equation and is solved exactly. We take a solution which behaves like the positive frequency mode in the flat spacetime in the past infinity for large wave number as a mode function for quantization. Assuming that the initial state of the scalar field is the vacuum state associated with this mode function, we obtain the power spectrum (figure 1). We will briefly disscuss the possible effect of curvature on the CMB fluctuation.

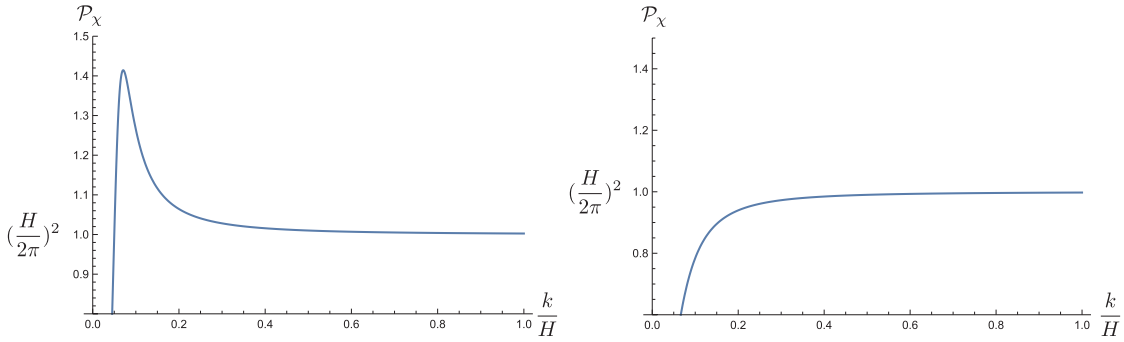

Figure 1: Power spectrum $\mathcal{P}_\chi(k/H)$ normalized by $(H/2\pi)^2$ for (left) negative curvature/(right) positive curvature.

First-principles studies of the effects of oxygen vacancies on the HfO_2-based ferroelectric tunnel junction

Jinho Byun[1], Taewon Min[1], Jaekwang Lee[*1]

[1] Department of Physics, Pusan National University, Busan 46241, Korea

Corresponding author. E-mail: Jaekwangl@pusan.ac.kr

Abstract:

Owing to the recent advances in the oxide growth technology, ferroelectricity has been stabilized even in a few nm-thick film, which makes it possible to realize the oxides-based ferroelectric tunneling junction (FTJ) combining the quantum-mechanical tunneling phenomena and switchable spontaneous polarization into novel device functionality. Among various ferroelectric oxides, HfO_2 is the most promising material for FTJ devices since it has the great advantage of complementary metal-oxide-semiconductor (CMOS) process compatibility. Despite this considerable attention, the influence of oxygen vacancies on the tunneling current has not been clearly understood yet. Here, using first-principles density functional theory calculations, we explored the role of interfacial oxygen vacancy on the tunneling current in the TiN/HfO_2/metal devices at the atomic scale. We find that the tunneling current in defective HfO_2 is enhanced by over three orders of magnitude compared to plain HfO_2 thin film. Our results show that the modulation of electronic properties via interfacial oxygen vacancy have a significant impact on HfO_2-based FTJ device performance.

This research was supported by the MOTIE (Ministry of Trade, Industry & Energy (#10080643) and KSRC (Korea Semiconductor Research Consortium) support program for the development of the future semiconductor device.

This work was also supported by the National Research Foundation of Korea (NRF) grant funded by the Korea government (2018R1A2B6004394)

Corrugation engineered out-of-plane polarization in 2D $MoTe_2$

Sera Jeon[1], Jaekwang Lee[1]

[1]*Department of Physics, Pusan National University, Busan, 46241, Korea*

E-mail: jaekwangl@pusan.ac.kr

In general, the coexistence of electric polarity and conducting characteristics is mutually exclusive because a finite band gap is critical to maintain the permanent electric dipole moment existing in the polar materials. Here, using the density functional theory calculation, we find the polar conducting feature can be developed in semiconducting monolayer 2H-$MoTe_2$ by generating corrugation. In particular, the out-of-plane polarization is observed even though crystallographically there exists only in-plane polarization. We expect our results contribute to finding optimal layered materials with giant out-of-plane polarization.

Emergence of Kondo Resonance in Graphene Intercalated with Cerium

Jinwoong Hwang[1], Kyoo Kim[2], Hyejin Ryu[1,3,4], Jingul Kim[5], Ji-Eun Lee[1], Sooran Kim[2,5], Minhee Kang[1], Byeong-Gyu Park[6], Alessandra Lanzara[7,8], Jinwook Chung[5,9], Sung-Kwan Mo[3], Jonathan Denlinger[3], Byung Il Min[5], and Choongyu Hwang[1,†]

[1] *Department of Physics, Pusan National University, Busan 46241, South Korea*

[2] *Max Planck-POSTECH/Hsinchu Center for Complex Phase Materials, Pohang University of Science and Technology, Pohang 37673, South Korea*

[3] *Advanced Light Source, Lawrence Berkeley National Laboratory, Berkeley, CA 94709, USA*

[4] *Center for Spintronics, Korea Institute of Science and Technology, Seoul 02792, South Korea*

[5] *Department of Physics, Pohang University of Science and Technology, Pohang 37673, South Korea*

[6] *Pohang Accelerator Laboratory, Pohang University of Science and Technology, Pohang 37673, South Korea*

[7] *Materials Sciences Division, Lawrence Berkley National Laboratory and Department of Physics, University of California, Berkeley CA 94720, USA*

[8] *Department of Physics, University of California, Berkeley CA 94720, USA*

[9] *Department of Physics and Photon Science, Gwangju Institute of Science and Technology, Gwangju 61005, South Korea*

The interaction of a magnetic impurity with surrounding electrons has been a long-standing theme in modern physics to understand fundamentals of many-body effects. In particular, antiferromagnetic screening of the local magnetic moment by conduction electrons leads to the formation of a new resonant-type many-body ground state, so-called Kondo resonance. Here we report the realization of the Kondo resonance in a prototypical two-dimensional system, graphene, induced by the presence of cerium with the localized spin of a $4f$ electron. The combination of two complementary techniques, angle-resolved photoemission spectroscopy and dynamic mean-field theory, reveals the development of new spectral weight near Fermi energy at lower temperature that is hybridized with the graphene π-band. The observed T-dependence provides not only a direct evidence of the formation of the many-body ground state in graphene, but also novel insight how Kondo physics emerges in the sea of two-dimensional Dirac electrons.

† corresponding e-mail: ckhwang@pusan.ac.kr

Odd-parity multipoles and magneto-current effect

Dept. of Phys., Hokkaido Univ.
M. Yatsushiro, S. Hayami

Multipoles have been used to represent anisotropic electric charge and current distributions in electromagnetic dynamics. Under the space-time inversion group, they are classified into four types: electric $[(\mathcal{P},\mathcal{T}) = ((-1)^l, +1)]$, magnetic $[(\mathcal{P},\mathcal{T}) = ((-1)^{l+1}, -1)]$, electric toroidal $[(\mathcal{P},\mathcal{T}) = ((-1)^{l+1}, +1)]$, and magnetic toroidal $[(\mathcal{P},\mathcal{T}) = ((-1)^l, -1)]$ multipoles where $\mathcal{P}$ and $\mathcal{T}$ are spatial- and time-reversal operations and l is the rank of multipoles. Recently, such multipoles have been applied to condensed matter physics, since they describe electronic degrees of freedom, such as charge, spin, and orbital in a systematic way [1][2]. Especially, the concept of multipoles has been developed in f-electron systems to describe strongly anisotropic nature, which results in findings of unconventional multipole orderings, e.g., electric quadrupole ordering in $PrIr_2Zn_{20}$ [3] and magnetic octupole ordering in $Ce_{1-x}La_xB_6$ [4]. They are also useful to understand and predict what types of physical responses and transport phenomena can occur. For example, magnetoelectric effect where the magnetization (electric polarization) is induced by external electric (magnetic) field can be caused with rank 0-2 multipoles activated in the absence of both spatial inversion and time-reversal symmetries: magnetic monopole, magnetic toroidal dipole, and magnetic quadrupole. However, systematic descriptions of odd-parity multipoles activated in noncentrosymmetric systems and their physical phenomena were still missing, since their formalism has not been completed.

In the present study, we focus on odd-parity multipoles and their magneto-current effect where the magnetization is induced by electric current in metal from the microscopic viewpoint [5]. By considering the multi-orbital system with different parities, e.g., p-d and d-f in the noncentrosymmetric tetragonal crystal, we investigate what types of odd-parity multipoles are activated. We find the key ingredients to lead to the magneto-current effect by examining the model: the spin-orbit coupling and the onsite and offsite hybridizations between orbitals with different parities. We show that the electric dipole degree of freedom is activated in the point group C_{4v} by the odd-parity hybridization. It is the origin of further unconventional physical phenomena, such as the magnetoelectric effect, once the magnetic toroidal dipole and magnetic quadrupole occurs through the electron correlation. We discuss how these cross-correlated phenomena are induced by the multipole orderings.

[1] Y. Kuramoto, H. Kusunose, and A. Kiss, J. Phys. Soc. Jpn. **78**, 072001 (2009).
[2] S. Hayami and H. Kusunose, J. Phys. Soc. Jpn. **87**, 033709 (2018).
[3] T. Onimaru, K.T. Matsumoto, Y.F. Inoue, K. Umeo, T. Sakakibara, Y. Karaki, M. Kubota, and T. Takabatake, Phys. Rev. Lett. **106**, 177001 (2011).
[4] R. Shiina, H. Shiba, and P. Thalmeier, J. Phys. Soc. Jpn. **66**, 1741 (1997)
[5] S. Hayami, M. Yatsushiro, Y. Yanagi, and H. Kusunose, arXiv: 1806.01964, (2018).

Study on the magnetic properties of π-electrons in the Anionic Magnetism of Rubidium Superoxide (RbO_2)

Fahmi Astuti[1,2], Mizuki Miyajima[3], Takeshi Kakuto[3], Takehito Nakano[4], Isao Watanabe[1,2] and Takashi Kambe[3]

RIKEN Nishina Center[1], Hokkaido University[2], Okayama University[3], Ibaraki University[4]

Alkalimetal superoxides, AO_2 (A= *Na, K, Rb, Cs*) are interesting materials to study in terms of their magnetic properties. The unpaired electron located in the π^* molecular orbital of the superoxide anion is responsible for the magnetic moment in this class of materials. This system also provides rare simple manifestations of the coupling between spin, lattice, and orbital degrees of fredom in the p-electron material [1]. In CsO_2, the structural phase transition prevails from high symmetry (tetragonal) to be lower symmetry (orthorombic) by decreasing of the temperature [2]. Furthermore, by the changing of the structure, the magnetic interaction is altered from paramagnetic to low-dimensional antiferromagnetic which leads a zig-zag like 1D chain along b-axis [3] followed by the formation of 3D long-range ordering below 10 K [4]. The evidence of low-dimensional magnetism in CsO_2 was also observed from high-field magnetization measurement [5].

In this presentation, I summarize the result of our investigation in RbO_2. Synchrotron X-ray diffraction data in RbO_2 shows the splitting of the peak indicating the existence of structural phase transition (detailed will be shown in the presentation). The first investigation of the microscopic magnetic nature of polycrystalline RbO_2 was carried out by using continuous muon beam. Our μSR data reveal the presence of long-range antiferromagnetic order at below about 15 K. The high-field magnetization in RbO_2 showed the absence of up-turn curvature. The results from current measurements indicate the three-dimensional magnetic interaction in this spin system.

References:

[1] E. R. Ylvisaker, R. R. P. Singh, and W. E. Pickett, *Phys. Rev. B* **81**, 180405 (2010)
[2] A. Zumsteg et al., *Phys. Cond. Matter* **17**, 267 (1974).
[3] S. Riyadi et al., *Phys. Rev. Lett.* **108**, 217206 (2012).
[4] F. Astuti et al, *to be published.*
[5] M. Miyajima, F. Astuti et al., *J. Phys. Soc. Jpn.* **87**, 063704 (2018).

Finite-size corrections to Fermi's golden rule

Yutaka Tobita
Hokkaido University of Science,
7-15-4-1 Maeda, Teine-ku, Sapporo 006-8585, Japan

Transition probability is one of the fundamental quantities that determines microscopic phenomena. In quantum theory, the Shrödinger equation determines the evolution in time of the states or the wavefunctions and a probability of a phenomenon is determined by the probability density i.e. the wavefunction. This is the principle of probability in quantum theory. The Fermi's golden rule or its extension the S-matrix are very popular formulae to calculate a transition rate or a cross section in quantum mechanics or quantum field theory. Students have already studied about them, of course [1]. They are used not only in physics but also chemistry and biology. This is because the golden rule provides an easy way to calculate the transition rate with plane wave states. However, that is just an approximation derived by Dirac in 1920s to calculate transition probability [2]. Recently, we studied about finite-size corrections to the golden rule and revealed that the corrections are not negligible in some phenomena where particles with very small masses such as neutrinos [3] or photons [4] are involved. In this talk, we will show
i) a brief review about the Fermi's golden rule and its finite-size corrections, and how to derive the transition probability in small time interval T as

$$P(T) = \Gamma T + P^d,$$

where P^d is a constant term from finite-size corrections.
ii) Application to neutrino physics [3] and photosynthesis [5]

These works are in collaboration with K. Ishikawa and N. Maeda (HU) and T. Yabuki (Hokusei Univ.)

References

[1] M. L. Goldberger and K. M. Watson, *Collision Theory*; L. I. Schiff, *Quantum Mechanics*; L. D. Landau and E.M. Lifshitz, *Quantum Mechanics*; M. E. Peskin and D. V. Schroeder, *An Introduction to Quantum Field Theory*; S. Weinberg, *The Quantum Theory of Fields I*; and there are many other good textbooks.

[2] P. A. M. Dirac, Pro. R. Soc. Lond. A 114, 243 (1927).

[3] K. Ishikawa and Y. Tobita, Prog. Theor. Exp. Phys. 2013, 073B02 (2013); Ann. Phys. 344, 118 (2014).

[4] K. Ishikawa, T. Tajima, and Y. Tobita, Prog. Theor. Exp. Phys. 2015, 013B02 (2015).

[5] N. Maeda, et. al, Prog. Theor. Exp. Phys. 2017, 053J01 (2017).

Plasmons in Atomic-scale/Nanoscale objects and Their Applications

Tadaaki NAGAO[1]

[1] *International Center for Materials Nanoarchitectonics,*
National Institute for Materials Science
**Email address: NAGAO.Tadaaki@nims.go.jp*

Abstract.

Surface plasmon polaritons and its low-dimensional variants as well as their confined standing waves (antenna resonances) have become increasingly important in nanotechnology since their optical properties are strongly dependent on the size and the shape of the small objects. Because the Fermi wavelength and screening length of most metals are at the nanometer scale, plasmons in metals are readily tuned by tailoring their shape, size, at the nanometer to the subnanometer scale. This closely relates to the purpose of nanotechnology which is to provide appropriate building blocks to embody nano-architecture with desired functions for novel electronics/photonics devices. The propagating modes of plasmon in open structures (surfaces, nanowires, etc.) can be studied by using electron spectroscopy and revealed a rich diversity of physics assocaiated with the electron dynamics. On the other hand, the localized resonating modes in closed structures (particles, finite-szed rods, etc.) strongly coulples with light and exhibit wide variety of applications in the field of nanophotonics, life science, and light harvesting technology. In this talk I present some fundamental aspects of confined plasmons in atomic-scale and nano-scale objects. Then I also show some applications in infrared sensing using boradband plasmonic absorbers, as wells as narrowband perfect absorbers.

References

[1] Tadaaki Nagao *et al., Sci. Technol. Adv. Mater.* **1**1 054506 (2010). http://iopscience.iop.org/1468-6996/11/5/054506|

[2] Jung-Sub Wi, Masud Rana, and Tadaaki Nagao, *Nanoscale* **4**, 2847-2850 (2012).

[3] J.-S. Wi, L.-K. Shrestha, and T. Nagao, " *Phys. Status Solidi RRL* **6**, 202-204 (2012).

[4] V. M. Silkin, T. Nagao, V. Despoja, J. P. Echeverry, S. V. Eremeev, E. V. Chulkov, and P. M. Echenique, Physical Review B **84**, 165416-1 -9 (2011). doi: 10.1103/PhysRevB.84.165416

[5] T. Nagao, "Chapter 9: Low-dimensional plasmons in atom sheets and atom chains," in Dynamics at Solid State Surfaces and Interfaces, Volume I, Edited by. U. Bovensiepen, H. Petek, M. Wolf (Wiley VCH), pp189-211(2010). ISBN: 978-3-527-40937-2

[6] T. Nagao, S. Yaginuma, T. Inaoka, and T. Sakurai, *Physical Review Letters* **97**, 116802-1 -4 (2006).

Vortex-charging in the Abrikosov lattice

Dept. of Phys., Hokkaido Univ.[1], *Dept. of Math. and Phys., Hirosaki Univ.*[2]
M. Ohuchi[1], **H. Ueki**[2] **and T. Kita**[1]

A number of studies on vortex-charging in type-II superconductors have been carried out based on the mean field theory of superconductivity such as the Bogoliubov–de Gennes (BdG) equations [1, 2]. However, the BdG equations have difficulties in identifying the forces responsible for the charging and also in incorporating Fermi-surface and gap anisotropies.

Recently, a study on the flux-flow Hall effect has been performed [3] based on the augmented quasiclassical equations in the Keldysh formalism with the Lorentz and pair-potential gradient (PPG) forces. On the other hand, we have derived the augmented quasiclassical equations in the Matsubara formalism with the Lorentz and PPG forces, and calculated the core charge of an isolated vortex using it [4]. Our results clarifies that the PPG force contributes dominantly to charging in the core region of an isolated vortex over a wide parameter range such as the temperature and magnetic-penetration-depth. However, the previous studies have also shown that the charge accumulation originating from the Lorentz force is enhanced substantially in finite magnetic fields [5]. This indicates that the Lorentz force contribution may become dominant over the PPG force contribution in finite magnetic fields.

We study the vortex-charging in the Abrikosov lattice due to the Lorentz and PPG forces to see which forces dominantly contribute to the charging in finite magnetic fields.

[1] M. Matsumoto and R. Heeb, Phys. Rev. B **65**, 014504 (2001).
[2] M. Machida and T. Koyama, Phys. Rev. Lett. **90**, 077003 (2003).
[3] E. Arahata and Y. Kato, J. Low Temp. Phys. **175**, 346 (2014).
[4] M. Ohuchi, H. Ueki, T. Kita, J. Phys. Soc. Jpn. **86**, 073702 (2017).
[5] W. Kohno, H. Ueki, and T. Kita, J. Phys. Soc. Jpn. **85**, 083705 (2016).

Fabrication and characterization of sputter iron-based film for energy applications

Hai Dang Ngo[1, 2], Thien Duc Ngo[1], Kai Chen[1,3], Akemi Tamanai[1], Orjan S. Handegard[1, 2], Naoto Umezawa[1], and Tadaaki Nagao[1,2].

[1]International Center for Materials Nanoarchitectonics, National Institute for Materials Science, Tsukuba 305-0044, Japan

[2]Department of Condensed Matter Physics, Graduate school of Science, Hokkaido University, Kita-10 Nishi-8 Kita-ku, Sapporo 060-0810, Japan

[3]Institute of Photonics Technology, Jinan University, Guangzhou, 510632, China

Abstract: Iron (III) titanates are composed of earth abundant elements and are attracting rapidly growing interest as highly promising candidates for the solar-energy applications such as photodegradation, solar-water splitting, and photovoltaics. In this article, we report a successful synthesis of orthorhombic pseudobrookite Fe_2TiO_5 thin films with RF sputtering followed by post deposition annealing in air at 550^{o}C. Chemical composition, crystal structure, surface morphology, and optical properties of the synthesized films were experimentally as well as theoretically characterized with X-ray diffraction (XRD), X-ray photoelectron spectroscopy (XPS), scanning electron microscope (SEM), atomic force microscope (AFM), Raman scattering spectroscopy, and UV-Vis absorption and DFT simulation. The film was confirmed to be single phase, and exhibited high-crystallinity orthorhombic pseudobrookite structure with a preferential crystal orientation of (331) with excellent adhesion on both glass and silicon substrates. Comparison of dielectric functions between spectroscopic ellipsometry and DFT simulation showed good matching. Estimated direct and indirect band gap values from the optical characterization also well understood in comparison with the energy band diagram from DFT simulations.

Keywords: Iron Titanate, Fe_2TiO_5, RF magnetron sputtering, optical properties, pseudobrookite, DFT calculation

The Electronic Specific heat in the Superconducting State of a Bismuth Sulfide Superconductor

Y. Wang, S. Takahashi, T. Suda, T. Tamura, H. Ohta, N. Momono

Muroran Institute of Technology, Muroran, 050-8585, Japan

In recent years, breakthrough discoveries have focused layered materials in the field of new superconducting materials. Especially the superconductivity in $LaO_xF_{1-x}BiS_2$ compounds attracted the attention of physicists. The characteristic structure is an alternate stacking of superconducting BiS_2 layers and blocking layers (LaO/F) for supplying electrons. The layered crystal structure is analogous to those of high-temperature (high-T_c) cuprate and Fe-based superconductors. The mechanism of the superconductivity in BiS_2 superconductors have not been clarified yet.

As is well known, the symmetry of the superconducting gap reflects the origin of the superconducting mechanism. The magnetic penetration depth measurements and specific heat measurements for the La-based and Nd-based BiS_2 superconductors have indicated the full gap with *s*-wave [1-3]. However, angle-resolved photoemission spectroscopy (ARPES) measurements suggested the large superconducting-gap anisotropy and attracted much attention [4]. Recently, the point contact spectroscopy measurements suggested the gap symmetry is unconventional pairing symmetry [5]. In order to clarify superconducting gap symmetry and bulk nature of superconductivity, we investigated the superconductivity by specific heat measurements.

Single crystals of $LaO_{1-x}F_xBiS_2$ (x = 0.5, 0.4) were grown by using CsCl/KCl-flux method under ambient pressure. The specific heat was measured in the temperature range of 0.3K~10K (PPMS). Shown in Fig. 1 is the temperature dependence of electronic specific heat. The electronic specific heat was obtained by subtracting the lattice contribution βT^3 from the total specific heat C (T). There is a clear jump that corresponds to the superconducting transition appeared in the x = 0.5. The presence of the jump clearly indicates the bulk nature of superconductivity. Besides, when x = 0.4, the jump is not clear. The transition area has become broadly. It's behavior expected the bulk like of superconductivity in this compound. In the low temperature, the data for x = 0.5 (red line) is going to zero, but the other line is uncertainty. At the same time, the T_c has got little suppression. For the x = 0.5 sample, it fits well with BCS theory and the energy gap is full gap with *s*-wave in weak-coupling limit.

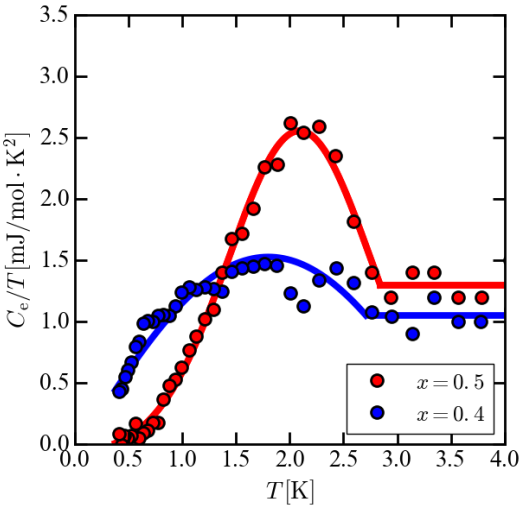

Fig. 1. *T dependence of electronic specific heat C_e/T*

References

[1] G. Lamura et al., Phys. Rev. B 88, 180509(2013)
[2] T. Yamashita et al., J. Phys. Soc. Jpn. 85, 073707 (2016).
[3] N. Kase et al., Phys. Rev. B 96, 214506(2017).
[4] Y. Ota et al., Phys. Rev. Lett. 118, 167002 (2017).
[5] F. Giubileo et al., J. Phys. Chem. Solids. 014 (2018).

Application of graphene and carbon nanotube -based heterostructures

Haeyong Kang[1], Jeongmin Park[2], Jeong-Gyun Kim[2], and Dongseok Suh[2]

[1]Department of Physics, Pusan National University, Busan 46241, Korea

[2]Department of Energy Science, Sungkyunkwan University, Suwon 16419, Korea

Carbon based materials have attracted significant attention, with structures of various dimensionalities such as, diamond and graphite in 3 dimension (3D), graphene in 2D, carbon nanotube (CNT) in 1D, and fullerene in 0D. Among them, we have systematically studied graphene and CNT for their interesting physics and possibility of wide application. In our studies, graphene conductance is found to be very sensitive to the change of the properties of oxide films underneath. The charge neutral point and quantum Hall states in graphene can be good indicators for probing the oxygen vacancy mechanism of thin film

In addition, I will also introduce the application and interesting properties of CNT sheets and yarns. CNT sheets were drawn from CNT forest where CNTs were grown densely and vertically. Free-standing CNT sheets consist of highly aligned but weakly entangled long bundles of CNT fibrils by van der Waals force without use of a binder. Due to their aerogel-like structure, CNT sheets show high flexibility, porosity and light weight, and can be stretched up to 600% on top of elastomer without damage of CNT sheets. Because the resistance does not vary during elongation-relaxation cycles, the application of stable stretchable conductor and high-performance heaters can be highlighted. Another strong point of CNT sheets is easy adaptation of other materials, which makes it possible to use as a flexible superconducting yarns.

An introduction to String Theory

Cristopher Arturo Chuñe Sosa[1]

[1] *Department of Physics, Hokkaido University, Sapporo, Japan*

One approach leading to the unification of quantum gravity and quantum field theory is by changing the way in which we describe the elementary particles. If instead of using the point-like description of particles, we state that these actually have some structure, i.e. as a one dimensional object called string, then the oscillation modes of the strings will be how we start formulating the particles of the standard model and the graviton. Consequences of this apparently trivial change also provide some solution to existing issues contained in field theory as well as some new features which can be treated with some mathematical ideas. In this opportunity, the fundamental ideas and features of the superstring theory will be presented in an intuitive way.

Single particle Raman scattering spectroscopy from nano/micro bismuth droplets on Si

Ørjan Sele Handegård[1,2], Masahiro Kitajima[1] and Tadaaki Nagao[1,2]
[1]International Center for Materials Nanoarchitectonics (MANA), National Institute for Materials Science (NIMS), 1-1 Namiki, Tsukuba, Ibaraki 305-0044, Japan
[2]Department of Condensed Matter Physics, Hokkaido University, Kita, Sapporo, Hokkaido 060-0808, Japan
E-mail: Tadaaki.Nagao@nims.go.jp

Abstract

Group V semimetals show exotic wavelength dependent optical response such as metal/dielectric duality, and offers unexplored possibilities in photonics and plasmonics research. There is a growing interest in bismuth (Bi), as it has many unusual properties, such as a Dirac-like band dispersion, smaller effective mass, very low carrier density, and longer mean free path compared to many other elemental metals. Majority of the works reported on Bi so far has mainly focused on bulk crystal or thin films.

In this presentation, we report the fabrication of single-crystalline nano/micrometer-sized well defined Bi hemispherical droplets and their structural and optical characterization using SEM, AFM, dark-field microscopy and confocal Raman microscopy. Bi droplets were formed by post-process annealing of an epitaxially grown Bi film in ultra high vacuum on Si(111). The crystallinity of the films and the subsequent droplet formation was monitored in situ by reflection high energy electron diffraction.

We observed that at the position of the pristine Bi droplets, the Si Raman signal (at 520 1/cm) from the substrate is reduced due to a shadowing/blocking effect by the Bi hemispheres. However, after exposing these Bi droplets to laser irradiation (785 nm, 30 mW/cm^2), the Si Raman signal becomes stronger at the Bi positions, compared to the intensities before laser exposure. The average relative enhancement factor showed a size dependence and ranged from 1.4-10.1 for a selection of droplets with increasing width. To our knowledge, this is the first time such a phenomenon is reported from a group V semimetal. The mechanism of Si phonon enhancement resembles SERS effect, but is not yet fully understood. We will continue investigating the correlation between the crystallinity, microfacets/roughness at the Bi surfaces, and light trapping/absorption effects together with the electromagnetic near-field enhancements.

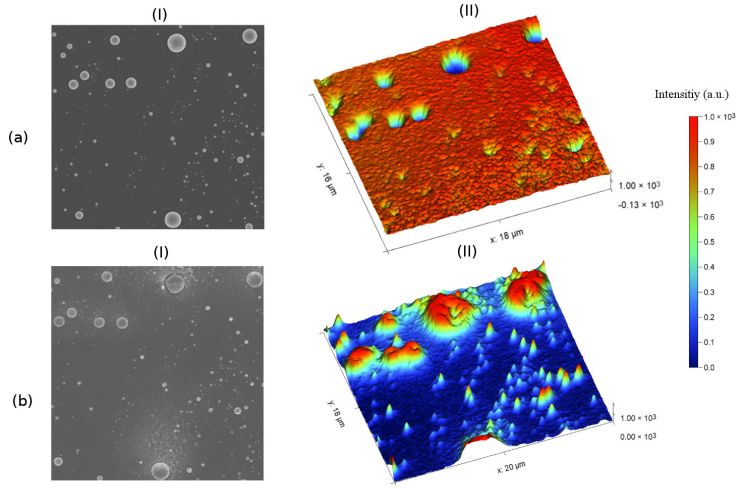

Figure 1. Effect of laser processing on Bi and Raman scattering. SEM image of Bi droplets (I) and Si 520 1/cm Raman mapping (II) before (a) and after (b) laser processing. Images are obtained from the same area.

electron-electron interaction in graphene decorated with ytterbium

Minhee Kang[1], Jinwoong Hwang[1], Ji-Eun Lee[1], Alexei Fedorov[2], and Choongyu Hwang[1*]

1 Department of Physics, Pusan National University, Busan 46241, Korea

2 Advanced Light Source, Lawrence Berkeley National Laboratory, Berkeley, CA 94201, USA

The presence of ytterbium leads to enhanced electron-phonon coupling in graphene strong enough to possibly realize superconductivity above ~1 K. The origin of the strong enhancement has been studied using angle-resolved photoemission spectroscopy. The electron band structure shows that of both heavily and lightly electron-doped graphene. The former shows the enhanced electron-phonon coupling compared to that of as-grown graphene, while the latter provides an evidence of enhanced electron-electron interaction. The strong enhancement of electron-phonon coupling in graphene decorated with ytterbium is attributed to the concomitantly enhanced electron-electron interaction.

The Study of Electronic Charge Order in a Bismuth Based Cuprate Superconductor Using Scanning Tunneling Microscopy/Spectroscopy

N. Momono[1], K. Kawamura[1], Y. Yokota[1], H. Ohta[1], T. Kurosawa[2], M. Oda[2], M. Ido[2]

[1]*Muroran Institute of Technology, Muroran, 050-8585, Japan*
[2]*Hokkaido University, Sapporo, 060-0808, Japan*

The superconducting transition temperature T_c is one of the most important parameters of superconductors. The T_c of high-temperature cuprate superconductors depends on hole concentration p. The typical p-dependence of T_c for cuprate superconductors is a dome-shaped T_c-p curve. The La-based cuprate superconductors such as $La_{2-x}Ba_xCuO_4$ and $La_{2-x-y}Nd_ySr_xCuO_4$ exhibit an anomalous "dip" feature near p~1/8 on the T_c-p curve, which is so-called "1/8 anomaly" of T_c. The 1/8 anomaly is due to the formation of a stripe structure with antiferromagnetic and charge orders. It is still unclear how the stripe order coexists with the High-T_c superconductivity in cuprates.

Recently it was reported in the scanning tunneling microscopy/spectroscopy experiments and the resonant X-ray scattering experiments that the checkerboad-like charge order occurs in $Bi_2Sr_2CaCu_2O_{8+\delta}$ (Bi2212), $Bi_2Sr_2CuO_{6+\delta}$ (Bi2201) and $YBa_2Cu_3O_7$ (YBCO) cuprate superconductors [1, 2]. In YBCO, it was also reported that the T_c plateau around T_c~60K is related to the appearance of the charge order. On the other hand, it was reported in Zn-doped Bi2212 that Zn-doping induces a dip feature on T_c-p curve [3], although there is no report about an anomaly on the T_c-p curve in pure Bi2212.

In the present study, we report that T_c is anomalously suppressed p~1/8 in $Bi_2Sr_2Ca_{1-x}Dy_xCu_2O_{8+\delta}$ (Dy-Bi2212). In the scanning tunneling microscopy/spectroscopy (STM/STS) experiments on Dy-Bi2212 with p~1/8, the checkerboard-like charge order appears at around a wave vector q_{CO}~0.3 rlu. In the STS spectrum, no well-defined coherent peak is observed. The dip of the T_c-p curve induced by the substitution of Dy in Bi2212 was similar to that observed in Zn-doped Bi2212, suggesting that the suppression of T_c near p~1/8 in Dy-Bi2212 is related to the pinning of the charge order.

References
[1] T. Kurosawa et al., Phys. Rev. B 81, 094519(2010), J. Phys. Soc. Jpn 85, 044709(2016).
[2] J. Chang et al., Nat. Phys. 8, 871 (2012)
[3] M. Akoshima et al., Phys. Rev. B 57, 7491(1998).

Observation of the chemical potential shift in SnSe by Ta adsorption

Ji–Eun Lee[1], Jinwoong Hwang[1], Minhee Kang[1], Kyoo Kim[2], Hyejin Ryu[2,3], Shujie Tang[3], Dung Anh Tuan[4], Sunglae Cho[4], Sung-Kwan Mo[3], Ho-soon Yang[1*], and Choongyu Hwang[1*]

*Email of corresponding authors: hsyang@pusan.ac.kr and ckhwang@pusan.ac.kr

[1]Department of Physics, Pusan National University, Busan 46241, South Korea

[2]Max Planck-POSTECH/Hsinchu Center for Complex Phase Materials, Pohang University of Science and Technology, Pohang 37673, Korea

[3]Advanced Light Source, Lawrence Berkeley National Laboratory, Berkeley, CA 94210, USA

[4]Department of Physics, University of Ulsan, Ulsan 680-749, South Korea

---

SnSe shows an excellent thermoelectric effect, of which efficiency (*ZT*) reaches up to 2.6 and 2.8 by hole and electron doping, respectively. The strong enhancement of *ZT* is attributed to multi-valley valence bands and strong anharmonicity of phonons. The former is responsible for the drastic change of charge carrier density upon substituting Sn with foreign atoms or creating Sn vacancies. Using angle-resolved photoemission spectroscopy, the change of charge carrier density has been investigated via the modification of the electron band structure of single crystal SnSe by foreign atoms. Tantalum adsorption results in the chemical potential shift by ~0.3 eV that roughly corresponds to the charge carrier density with maximum *ZT*. This result suggests an alternative way to control the thermoelectric effect that will provide a viable route towards the realization of high thermoelectric performance.

Magnetic proximity effect in $Nd_{1-x}Sr_xMnO_3$ multilayers

SangKyun Ryu[1], Hyegyeong Kim[2], Jinhyung Cho[3], Hyoungjeen Jeen*[1]

[1]*Department of Physics, Pusan National University, 46241*

[2]*Core Research Facilities, Pusan National University, 46241*

[3]*Pusan National University, Department of Physics Education, 46241*

Abstract

It is well-known that the change of stoichiometry changes physical properties easily in manganites. We grew two kinds of $Nd_{1-x}Sr_xMnO_3$ thin films with different stoichiometry by oxygen partial pressure control. We grew multilayers by stacking foregoing $Nd_{1-x}Sr_xMnO_3$ with differently hole-doped $Nd_{1-x}Sr_xMnO_3$ (x ~ 0.5 and 0.3) as sublayers. The formation of multilayers without change of lattice constants is confirmed by x-ray diffraction. Detailed magnetic characterization shows the enhancement of magnetic moments in multilayers to comparing with single layer. Also, when the thickness of each layer is decrease in multilayers, magnetic moment of multilayers is more enhanced. This result clearly indicates smearing of ferromagnetism into the less-magnetic layers at the interfaces. We suggest polarized neutron reflectivity experiment to approve the role of interface at multilayer films. This interfacial magnetism is useful to design magnetic oxides with high magnetic moments. This work was supported by the Basic Science Research Program through the National Research Foundation of Korea (NRF) funded by the Ministry of Education (NRF-2015R1D1A1A02062175).

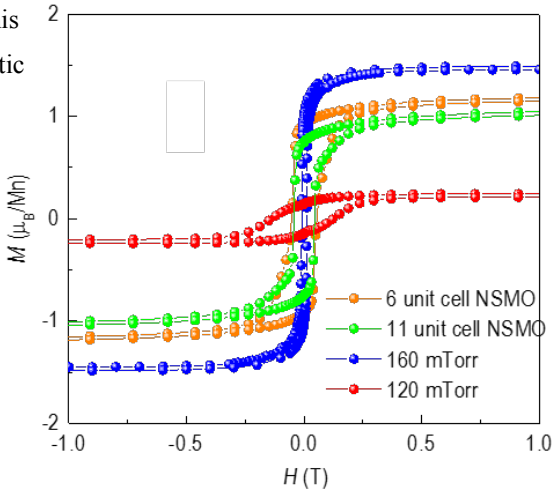

Enhancement of magnetic properties in M-type Sr-hexaferrite

Lien Phuong Nguyen, Jaekwang Lee

Department of Physics, Pusan National University, Pusan 46241, Korea

Hexagonal strontium hexaferrite ($SrFe_{12}O_{19}$) is commonly used as permanent magnets. Recently, there have been many attempts to further enhance the magnetic properties of Sr-hexaferrite with various cationic substitutions. Here, using the a first-principles density functional theory calculations, we studied the effect of co-doping with Ca-X (X = La, Gd, Y, Al) on the electronic property and total magnetic moment in $Ca_2XSr(Fe_{12}O_{19})_4$. The initial result shows a little change in the total magnetic moment of the $Ca_2XSr(Fe_{12}O_{19})_4$, which comes from the magnetization enhancement in Fe^{3+} sites due to the redistribution of excess charge brought by the dopant.

Contribution of Quantum Effects on the Muon Site Calculation of La_2CuO_4

M. R. Ramadhan[1,2], I. Ramli[1,3], M. D. Umar[1,3], S. Winarsih[1,2], B. Adiperdana[1,5], B. Kurniawan[2], M. I. Mohamed-Ibrahim[4], S. Sulaiman[4], T. Adachi[6], I. Watanabe[1,2,3,4]

[1]*Meson Science Laboratory, RIKEN Nishina Center, Wako 351-0198, Japan*
[2]*Department of Physics, Universitas Indonesia, Depok 16424, Indonesia*
[3]*Department of Condensed Matter Physics, Hokkaido University, Sapporo 060-0810, Japan*
[4]*School of Distance Education, Universiti Sains Malaysia, Penang 11800, Malaysia*
[5]*Department of Chemistry, Universitas Padjajaran, Sumedang 45363, Indonesia*
[6]*Department of Engineering and Applied Sciences, Sophia University, Tokyo 102-8554, Japan*

The muon spin relaxation (μSR) method is a powerful tool to investigate electronic states of the Cu-based high-T_C superconducting oxides. To get a better understanding of the magnetically ordered state of La_2CuO_4 (LCO), muon positions information is required. Although several attempts have been made in the past, any unified methods to investigate muon positions have not yet been firmly established. For this reason, the μSR results achieved on LCO, even in the early stage of the high-T_C history, have not yet been fully explained [1-3]. We are approaching this matter by using the density functional theory (DFT) calculation method. The on-site Coulomb repulsion energy, U = 8 eV, was taken into account to include the correlation energy between the *3d* orbitals of neighboring Cu atoms. Three minimum potential positions were estimated from the calculations and set to be the initial muon-stopping positions. In subsequent calculations, one muon, which effectively act as a dilute charged impurity, was introduced into a supercell structure. The supercell contains 32-unit cells formed by the inclusion of 4-unit cells along *a* and *b*-axis, and 2 cells along *c*-axis. The supercell structure was then relaxed until the forces between the ions are below convergence threshold. From our current results, the magnetic moment on the nearest Cu atom in the perturbed system was slightly lowered by the presence of muon, while the rest of the magnetic moment shows a relatively similar value with the unperturbed system. This local deformation caused by the muon was taken into account along with the zero-point vibration motion of muon to calculate dipole fields at the muon positions. The results of our investigations will be presented.

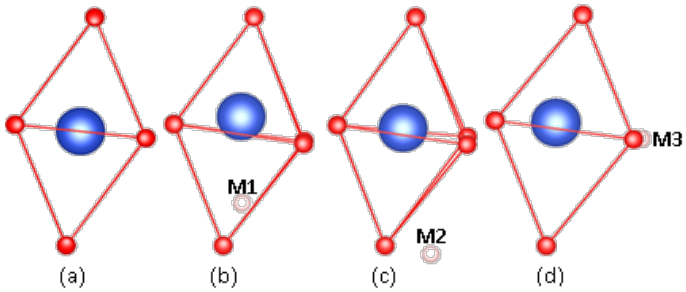

Fig. 1: *Comparison of CuO_6 octahedra after the relaxation of lattice structure and the muon position in the case of (a) without the muon and putting the muon at initial minimum potential positions of (b) M1, (c) M2 and (d) M3.*

References

[1] R. Saito *et al.,* Physica C **185-189**, 1217 (1991).
[2] S. B. Sulaiman *et al.*, Phys. Rev. B **49**, 9879 (1994).
[3] H. U. Suter *et al.*, Physica B **326**, 329 (2003).

New π-d interaction systems in the organic conductors

Noriaki Matsunaga,

Department of Physics, Hokkaido University
Email: mat@phys.sci.hokudai.ac.jp

The *π-d* interacting system has been has been one of the most attractive topics in the organic conductors. Especially, the *π-d* interacting system λ-$(BETS)_2FeCl_4$ becomes an antiferromagnetic (AF) phase at zero magnetic field and a field induced superconductivity above 17 T [1], which is explained by the Jaccarino-Peter compensation mechanism [2]. In contrast, λ-$(BETS)_2GaCl_4$ shows metal-superconductivity transition at 5.5 K [3]. Therefore, the AF phase of λ-$(BETS)_2FeCl_4$ is thought to be induced by the existence of 3*d* spins of the $FeCl_4$ anion. On the other hand, λ'-$(BETS)_2GaBr_4$ shows the metal-insulator transition at 50 K with magnetic anomaly [4]. To clarify the role of the 3*d* spins and the *π-d* Interaction in the λ- and λ' salts, we investigate quasi-two dimensional organic conductors λ-$(BEDT\text{-}STF)_2GaCl_4$, λ-$(BEDT\text{-}STF)_2FeCl_4$, λ'-$(BEDT\text{-}STF)_2GaBr_4$, and λ'-$(BEDT\text{-}STF)_2FeBr_4$.

From the resistivity measurements under pressure and magnetic field, we found that the λ- and λ'-BEDT-STF salts are located at the lower pressure region than the λ- and λ'- BETS salts. Figure 1 shows the universal phase diagram of λ-type family. λ-$(BEDT\text{-}STF)_2GaCl_4$ does not show the AF phase at ambient pressure even though it shows the strong AF interaction [5]. On the other hand, λ-$(BEDT\text{-}STF)_2FeCl_4$ shows the AF transition in the π-spin system at 16 K [6]. These results suggest that the AF state of the π-electron system in the BEDT-STF layers is stabilized by the 3d spins on $FeCl_4$ anions through the *π-d* interaction. The magnetic susceptibility of λ-$(BEDT\text{-}STF)_2FeCl_4$ at ambient pressure can be fit the AF ordered π-spin model [7]. Therefore, the ground state of λ-$(BEDT\text{-}STF)_2FeCl_4$ at ambient pressure is thought to be the AF ordered state. Moreover, the relation between the static susceptibility and the splitting of the NMR shift suggests the existence of the relatively strong *d−d* AF interaction. Therefore, the *π-d* and *d-d* interactions show the significant role in the ground state of this pressure region of λ-type family.

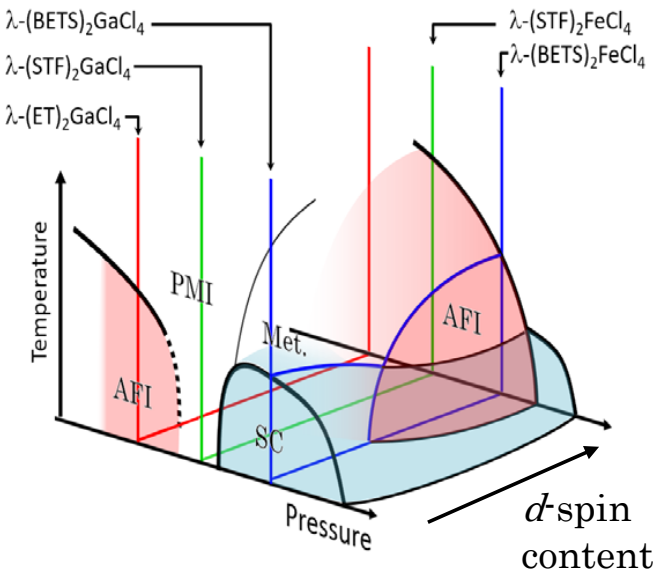

Fig. 1. Universal phase diagram of λ-type family.

References

[1] Uji, S. *et al. Nature*., **410**, 908 (2001).
[2] V. Jaccarino and M. Peter, *Phys. Rev. Lett*., **9**, 290 (1962).
[3] H. Kobayashi, *et al. Chem. Lett*., **22** 2179, (1993).
[4] Tanaka, H. *et al. Chem. Lett.*, **28** 133 (1999).
[5] Minamidate, T. *et al*. *JPSJ*, **84**, 063704 (2015).
[6] Minamidate, T. *et al*. Phys. Rev. B **97**, 104404 (2018)
[7] Akiba, H. *et al. JPSJ*, **80**, 063601 (2011).

Study of Microscopic Magnetism in $YBa_2Cu_3O_6$ by μSR and DFT

Irwan Ramli[1,2], S. S. Mohd-Tajudin[3], M. R. Ramadhan[1,4], M. I. Mohamed-Ibrahim[3], S. Sulaiman[3], T. Nishizaki[5], B. Kurniawan[4], and I. Watanabe[1,2,3,4]

[1]*Meson Science Lab., RIKEN Nishina Center, 2-1 Hirosawa, Saitama 351-0198, Japan,*
[2]*Department of Condensed Matter Physics, Graduate School of Science, Hokkaido University, Kita-ku, Sapporo 060-0810, Japan,*
[3]*Computational Chemistry and Physics Laboratory, School of Distance Education, Universiti Sains Malaysia, Penang 11800, Malaysia,*
[4]*Department of Physics, Universitas Indonesia, Depok 16424, Indonesia,*
[5]*Department of Electrical Engineering, Kyushu Sangyo University, Fukuoka 813-8503, Japan.*

The antiferromagnetic (AF) interactions in Cu-based high-T_C superconductors is the key to understand the mechanism of high-T_C superconductivity. $YBa_2Cu_3O_6$ ($YBCO_6$) is the mother system of the Y-system high-T_C superconductor. This system is well known as Mott insulator with the long-range AF ordering with T_N = 350 K.[1] The AF ordering disappears with increasing doped holes introduced by additional oxygen and the superconductivity appears.[2] We utilized the muon-spin relaxation (μSR) technique to study the microscopic electronic and magnetic properties of $YBCO_6$. The μSR is extremely sensitive to probe the local magnetism due to the large gyromagnetic ratio of the muon spin.[3] But it has difficulties in investigating quantitative information of hyperfine interactions due to the unknown positions of the injected muons in the materials and complicated local perturbation caused by the muons to its surroundings.[4]

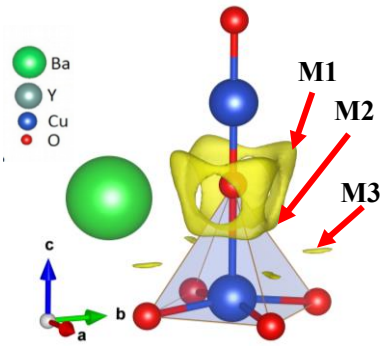

Fig. 1: Possible initial muon stopping positions in $YBCO_6$ estimated from our DFT calculations. The yellow area indicates the isosurface at 500 meV.

We are developing research method to address those issues by using density functional theory (DFT) calculations. As the muon has positive charge, it prefers to stop at a local minimum potential position in materials. We found three possible initial muon sites in $YBCO_6$ marked as M1, M2 and M3 as shown in Fig. 1. In order to investigate local perturbations caused by the muon as a dilute charged impurity, we modeled a supercell which contains 32 unit cells, 4 unit cells along a- and b-axis and 2 unit cells along c-axis, and only one muon. We then calculated relaxations of the atomic positions throughout the whole the supercell. We also included changes in the local electronic states and the spatial distribution of spin density of surrounding electrons. Taking into account the zero-point vibration energy of the muon, and comparing with μSR experimental data, we reveal information about muon positions and its surrounding electronic state.

References

[1] J. M. Tranquada *et al.*, Phys. Rev. B **38**, 2477-2485 (1988).
[2] Y. Koike *et al.,* J. Phys. Soc. Jpn. **85**, 091006 (2016).
[3] S. Sanna *et al*., Phys. Rev. Lett. **93**, 2017001 (2004).
[4] J. S. Möller *et al.*, Phys. Scr. **88,** 068510 (2013).

Magnetically ordered states in hole-doped pyrochlore iridate $Y_2Ir_2O_7$

J. Angel[1, 2], H. Nomura[3], T. Taniguchi[3], K. Matsuhira[3], I. Watanabe[1, 2]
[1]RIKEN Nishina Center, [2]Hokkaido University, [3]Kyushu Institute of Technology

Pyrochlore iridates, $R_2Ir_2O_7$ (R= Y and lanthanides), are worthy to be studied because of its frustrated magnetic interactions. $Y_2Ir_2O_7$ is predicted to be a Weyl semimetal followed by the metal-insulator transition (MIT) around 170 K and with an all-in all-out magnetic ground state [1,2]. Since the Y atom does not possess a local magnetic moment, the magnetic properties of Ir moment which play an important role in exotic electronic states in $R_2Ir_2O_7$ can be directly investigated. Moreover, the hole-concentration dependence on the magnetic properties can be clarified including a quantum critical behavior from the semiconducting to metallic states [3].

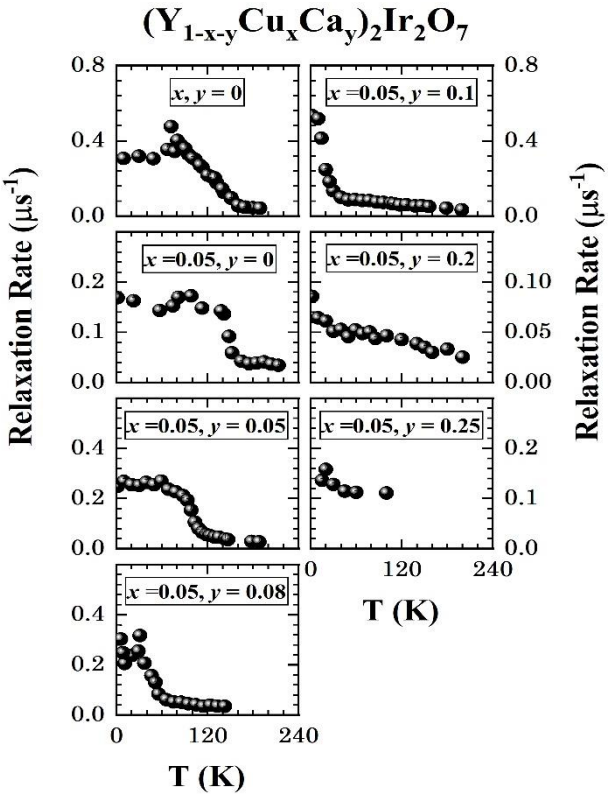

Figure 1. Zero-field time spectra of $Y_2Ir_2O_7$ and its hole-doped compounds.

The MIT of $(Y_{1-y}Cu_xCa_y)_2Ir_2O_7$ at variable y fixing x which involves the antiferromagnetic transition is suppressed compared to that observed in the non-doped sample by Cu- and Ca-doping. In order to approach to investigate magnetically ordered states of hole-doped $Y_2Ir_2O_7$, I applied the muon-spin relaxation method. Figure 1 shows the temperature dependence of the muon-spin relaxation rate measured at $(Y_{1-y}Cu_xCa_y)_2Ir_2O_7$. Changes in the magnetic properties and a phase diagram as the effect of Cu and Ca substitution will be discussed.

References:
[1] W. K. Zhu *et al.,* Phys. Rev. B **90**, 054419 (2014).
[2] H. Fukazawa and Y. Maeno, J. Phys. Soc. Jpn. **71**, 2578 (2002).
[3] L. Savary, E. Moon and L. Balents., Phys. Rev. X **4**, 041027 (2014).
[4] W. Witczak-Krempa et al., Cond. Matter. Phys. **5**: 57-82 (2014).
[5] S.M. Disseler *et al*., Phys. Rev. B **86**, 014428 (2012).

Manipulating artificial plasmonic heterostructures to control spectrally selective absorption and emission in the infrared region

Tung Anh Doan[1, 2], Thang Duy Dao[1], Satoshi Ishii[1] and Tadaaki Nagao[1,2].

[1]International Center for Materials Nanoarchitectonics, National Institute for Materials Science, Tsukuba 305-0044, Japan

[2]Department of Condensed Matter Physics, Graduate school of Science, Hokkaido University, Sapporo 060-0810, Japan

Abstract: The optical properties of natural materials essentially depend on their chemical compositions rather than their sample sizes. Artificial plasmonic heterostructures are made up of ensembles of sub-wavelength building blocks known as meta-atoms. These artificial materials reveal a different and fascinating picture: manipulation of geometrical parameters and arrangement of meta-atoms changes their optical properties dramatically. In this work, we demonstrate the ability to control spectrally selective IR absorption and emission by coupling the fundamental electric-magnetic resonance mode of a metal-insulator-metal (MIM) disk array resonator and incident waves. As a proof of concepts, a MEMS-based hybrid multi-color plasmonic-pyroelectric infrared detector was demonstrated experimentally to selectively absorb IR radiation at 3.5, 3.9, 4.3 and 4.7 μm. Alternatively, we also fabricated a spectrally selective multi-color thermoelectric detector, which combines the concepts of a MIM disk array resonator and a Si-based thermoelectric transducer to selectively absorb IR radiation at 3.5, 3.9, 4.3 and 4.7 μm. However, these subwavelength patterned structures require high-precision and multi-step lithography, which poses many challenges for fabrication on large scale or curved surfaces. To overcome this problem, we proposed to couple incident IR light at very narrow absorption band utilizing planar asymmetric Fabry-Perot cavities in two forms: plain metal-dielectric-metal (MDM) and [distributed Bragg reflector]-dielectric-metal (DDM). As a proof of concept, we realized an Au-Al_2O_3-Au based spectrally selective emitter and a hybrid 3(SiO_2-Si)|SiO_2|Al-based pyroelectric detector with high-resolution spectroscopy, flexible tunability, and lithography-free fabrication. For practical applications, spectrally selective multi-color detectors can be used in pyrometry to yield accurate temperature measurement of non-greybody objects. Inherent emissivity characteristic of non-greybody objects is one of the most challenging parameters to manage to ensure accurate temperature measurement. However, the usage of a pre-determined emissivity value or analytic fitting functions often leads to unexpectedly catastrophic temperature errors. To circumvent this problem, we proposed a novel approach using artificial intelligence (AI) algorithm, specifically artificial neural networks, This approach promises to extract the true temperature of non-gray surfaces from multi-color pyrometers with much higher accuracy.

Keywords: plasmonic, meta-atom, spectrally selective, emitter, detector, multicolor pyrometry, temperature-emissivity separation, artificial neural network

Exploring Optical and Thermal Properties of Non-noble Metal Plasmonic Structures

Manpreet Kaur[1,2], Satoshi Ishii[1*], Satish Laxman Shinde[1], Thang Duy Dao[1] and Tadaaki Nagao[1,2*]

[1]International Center for Materials Nanoarchitectonics (MANA), National Institute for Materials Science (NIMS), Tsukuba, Ibaraki, 305-0044, Japan

[2]Department of Condensed Matter Physics, Hokkaido University, Sapporo, Hokkaido, 060-0810, Japan

Non-noble metal plasmonic materials have been attracting significant attention both in applied and fundamental researches. For example, titanium nitride (TiN) is a typical refractory ceramic and is attracting significant interest for photothermal applications in industry. Gallium (Ga) nanostructures is also drawing attention as temperature-tuneable plasmonic element operative in the ultraviolet to the infrared region. The lossy plasmonic resonance of TiN nanoparticle are broad enough to cover visible to near infrared region of the solar spectrum. We have fabricated solar-heat converting devices with titanium nitride nanoparticles loaded on ceramic wool and in porous alumina for floatable water distillation devices and achieved high photothermal performances [1] [2]. Among the ultraviolet materials, gallium stands out for its complementary material properties compared with the noble metal nanoparticles (NPs) [3]. Unlike Au or Ag, Ga has a Drude-like dielectric function extending from the vacuum ultraviolet through the visible and, in the liquid state, into the infrared spectral region. The experiment and electromagnetic simulation are combined to study the optical response of a single Ga nanostructures (nanoparticles and nanowires) of various diameters and length based upon its temperature-dependent optical constants.

This study experimentally suggests the use of non-noble metal plasmonic materials based upon the previous theoretical predictions of plasmonic behaviour of TiN and Ga.

[1] S. Ishii, R. P. Sugavaneshwar, T. Nagao, The Journal of Physical Chemistry C 2015.
[2] M. Kaur, S. Ishii, S. L. Shinde, T. Nagao, ACS Sustainable Chemistry & Engineering 2017, 5, 8523.
[3] M. W. Knight, T. Coenen, Y. Yang, B. J. Brenny, M. Losurdo, A. S. Brown, H. O. Everitt, A. Polman, ACS nano 2015, 9, 2049.

(2) Poster Presentations

24th of July
@Academic rounge 1 & 2 in the faculty of engineering (10:50 ~ 12:10)

Competing magnetic phases emerged under magnetic field in triangular lattice dimer $Cs_3Fe_2Cl_9$

[1]Y. Ishii, [2]Y. Matsushita, [1]H. Yoshida, [1]M. Oda, [3]M. Hagihala, [4]T. Masuda, [5]T. Kida, [5]Y. Narumi, and [5]M. Hagiwara.

[1]*Dept.of Phys.Grad.Sch.Sci., Hokkaido Univ.*, [2]*National Institute for Material Science*, [3]*KEK − IMSS*, [4]*ISSP*, [5]*AHMF.Dept.of Phys.Grad.Sch.Sci.Osaka Univ.*

$A_3M_2X_9$ has the crystal structure which contains triangular lattices consist of the M ion dimers, and the triangular lattices stack along the c-axis in a hexagonal stacking manner (Figure 1(a)). In $A_3M_2X_9$, there are three interactions J_0 (intra-dimer interaction), J_p (inter-dimer interaction within the triangular layer) and J_c (inter-dimer interaction between the triangular layers) as shown in the Figure 1(b) and (c). The competition of these interactions often evokes interesting magnetisms including magnetization plateau and spin singlet ground state [1-4]. In the previous study of $Cs_3Fe_2Cl_9$, only the magnetic susceptibility of the powder sample was reported, therefore, the ground state of $Cs_3Fe_2Cl_9$ has not been understood well yet [5]. We succeeded synthesizing the single crystals of $Cs_3Fe_2Cl_9$, and we studied the magnetic properties of the compound by means of a magnetic susceptibility, a heat capacity, a high field magnetization and an elastic neutron scattering on the single crystals. The magnetic susceptibility revealed that $Cs_3Fe_2Cl_9$ was $S = 5/2$ antiferromagnet (AFM) (Θ_W = - 20.1 K), and our analysis indicated antiferromagnetic J_0 = - 2.3 K and the average of the out of dimer interactions $J_p + J_c$ = - 0.7 K were comparable with each other. The magnetic susceptibility exhibited a sudden drop at $T_N = 5.3$ K below 1 T at which a very steep peak appeared in the heat capacity. The sharpness of the anomalies indicates that a 1st order transition occurs at T_N. We found that the magnetic state below T_N was quite sensitive to magnetic field. Under the magnetic field applied parallel to the c-axis, $Cs_3Fe_2Cl_9$ shows field induced successive phase transitions such as meta-magnetic transitions with hysteresis and $M_S/2$ magnetization plateau, which is probably due to the comparable energy scale of the J_0, J_p, J_c, spin anisotropy, and magnetic field. Finally, we obtained the rich $H - T$ magnetic phase diagram under H // c-axis as summarized in Figure 1(d). The neutron diffraction in the zero-magnetic field revealed that the ground state was the stripe type magnetic ordered state which was same as the spin structure of the ground state of the buckled honeycomb lattice AFM Ba_2NiTeO_6 [6].

Therefore, $Cs_3Fe_2Cl_9$ is regarded as buckled honeycomb AFM rather than the triangular lattice dimer system magnetically. In my presentation, I will introduce the detail experimental results and discuss the interesting magnetic properties of $Cs_3Fe_2Cl_9$.

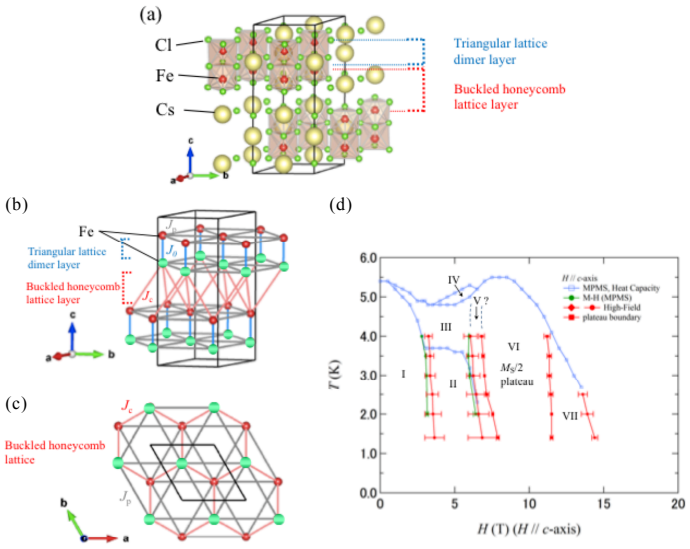

Fig. 1: (a)The perspective view of the crystal structure of $Cs_3Fe_2Cl_9$. (b)(c)The magnetic interaction passes in $Cs_3Fe_2Cl_9$. (d) $H - T$ magnetic phase diagram of $Cs_3Fe_2Cl_9$.

References

[1] B Leuenberger *etal.*, Chem. Phys. Lett. **1**26, 255-258 (1986).

[2] B Leuenberger *etal.*, Inorg. Chem. **2**5, 2930-2935 (1986).

[3] B Leuenberger *etal.*, Solid State Chem. **6**4, 90-101 (1986).

[4] T. Ziman *etal.*, Phys. Soc. Jpn. **7**4, 119-128 (2006).

[5] A. P. Ginsberg *etal.*, Inorg. Chem. **2**, 817-822 (1963).

[6] S. Asai *etal.*, Phys. Rev. B **9**3, 024412 (2016).

Ground-State Wave Function of the Fermion-Boson Mixtures with Fermion-Boson Interactions

Dept. of Phys., Hokkaido Univ.

W. Kouno and T. Kita

Quantum statistical physics on the basis of second quantization is the most fundamental idea for considering many-body systems. This method is supported by the assumption that the considering system is composed of same particles with permutation symmetry (bosons) or antisymmetry (fermions). On the other hand, there also exist mixed systems with different kinds of particles. In such systems, many-body correlations between different particles bring about nontrivial phenomena, such as superconductivity induced by electron-phonon coupling[1].

In superconductors, superfluidity appears in the system with emergence of a well-defined macroscopic phase, which originates from the macroscopic particle-number fluctuation. Although the existence of the macroscopic phase can be observed through the DC Josephson effect[2-4], the origin of the particle-number fluctuation is not clear in isolated systems. Recently, a variational wave function of superconductors has been constructed, which incorporate the correlation effects between Cooper pairs beyond BCS theory[5]. According to the study, the correlations produce finite non-condensed particles in the ground state, consequently, the fluctuation of the number of Cooper pairs occurs naturally.

In this presentation, we construct the variational ground-state wave function of weakly interacting homogeneous fermion-boson mixtures with particle-number-conserving manner. Using the ground state, we show the following topics. (1) The fermion-boson interaction induces quantum depletion of the BEC. (2) The quantum depletions interact with fermions and give rise to the momentum-emission (-absorption) processes of fermions in the same way as electron-phonon coupling. (3) The ground-state is given as a superposition over different particle-number of states even in the number-fixed systems. Therefore, superconducting state with well-defined macroscopic phase may appear naturally even in the number-fixed fermions due to the fermion-boson interactions. We also show the numerical results assuming the system is a dilute atomic gas. We discuss the nature of the ground state quantitatively by showing the results of ground-state energy, quantum depletions, and pair potential of fermions.

[**1**] J. Bardeen, L. N. Cooper, and J. R. Schrieffer, Phys. Rev. **106**, 162 (1957).

[**2**] B. D. Josephson, Phys. Lett. **1**, 251(1962)

[**3**] V. Ambegaokar, and A. Baratoff, Phys. Rev. Lett. **10**, 486 (1963).

[**4**] P. W. Anderson, and J. M. Rowell, Phys. Rev. Lett. **10**, 230 (1963).

[**5**] X. Si, WK, and T. Kita, submitting

Magnetization measurement of $Ce(Ru_{1-x}Rh_x)_2Al_{10}$ ($x < 0.05$) under Electric Current

N. Shikanai[1], M. Yamamoto[1], A. Kohriki[1], H. Hidaka[1], T. Yanagisawa[1], H. Amitsuka[1], H. Saito[2], C. Tabata[3], H. Tanida[4], T. Matsumura[5], and M. Sera[5]

[1] *Graduate School of Science, Hokkaido Univ., Sapporo 060-0810, Japan*
[2] *KENS IMSS KEK, Naka 319-1106, Japan*
[3] *PF IMSS KEK, Tsukuba 305-0801, Japan*
[4] *Liberal Arts and Sciences, Toyama Pref. Univ., Imizu 939-0398, Japan*
[5] *ADSM, Hiroshima Univ., Higashihiroshima 739-8530, Japan*

Toroidal moment $\boldsymbol{t}$ is one of the parameters that describe strength of the magnetoelectric coupling. According to a theoretical prediction by S. Hayami *et al.*, the toroidal moment can be active even in metallic systems, where the occurrence of exotic phenomena, such as magnetization induced by electric current, is expected [1]. Recently, we experimentally found the electric current-induced magnetization in an antiferromagnetic (AFM) ordered state of a metallic system UNi_4B [2]. However, the observed magnetoelectric effects in UNi_4B cannot be explained in part by the theoretical model. Further investigation in other metallic systems with the toroidal moment is required for full understanding of the magnetoelectric effect.

We now focus our attention on another AFM metallic system $CeRu_2Al_{10}$ and its Rh-doped system $Ce(Ru_{0.95}Rh_{0.05})_2Al_{10}$. They crystallize into $YbFe_2Al_{10}$-type orthorhombic structure with *Cmcm* (D_{2h}^{17}, No. 63), where Ce ions align along *c*-axis forming zigzag structure, with no local inversion symmetry. Magnetic moments of the Ce ions order antiferromagnetically pointing to the *c*-axis at $T_N = 27$ K for $CeRu_2Al_{10}$, while the magnetic moments of $Ce(Ru_{0.95}Rh_{0.05})_2Al_{10}$ point to the *a*-axis with the AFM ordering below $T_N = 24$ K [3,4]. Both AFM orders have same propagation vector of $\boldsymbol{q} = (0, 1, 0)$. In the present study, dc *M* measurements under electric current for each setting of $\boldsymbol{I} \parallel a$ and *c*, and $\boldsymbol{H} \parallel a$, *b*, and *c* have been performed using large single crystalline samples provided by H. Tanida. Figure 1 shows the temperature dependence of *M* under $\boldsymbol{I}$ for $CeRu_2Al_{10}$. It is found that the additional *M* (ΔM) is induced by applying electric current below T_N for the three settings: $(\boldsymbol{I}, \boldsymbol{H}) \parallel (a, c)$, (c, a), and (c, b). Similar ΔM are also observed in $Ce(Ru_{0.95}Rh_{0.05})_2Al_{10}$. We are going to discuss about the cause of the observed magnetoelectric effects in these compounds based on the concept of odd-parity multipoles.

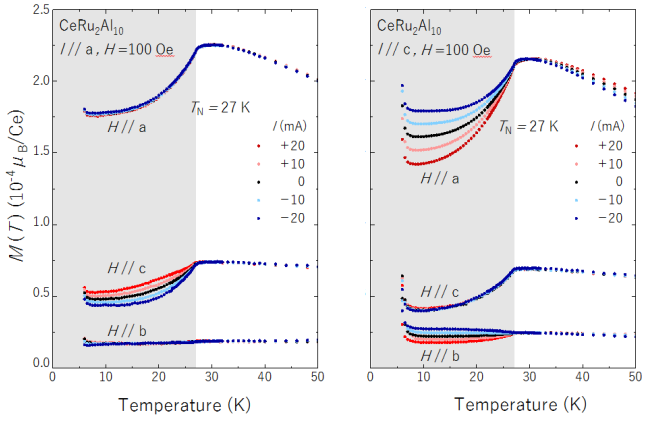

Fig. 1. Temperature dependence of *M* under electric current at $\boldsymbol{H} = 100$ Oe for $CeRu_2Al_{10}$. (left) $\boldsymbol{I} \parallel a$, and $\boldsymbol{H} \parallel a$, *b*, and *c*; (right) $\boldsymbol{I} \parallel c$, and $\boldsymbol{H} \parallel a$, *b*, and *c*.

References

[1] S. Hayami, H. Kusunose, and Y. Motome, Phys. Rev. B **90**, 024432 (2014).
[2] H. Saito, *et al.*, J. Phys. Soc. Jpn. **87**, 033702 (2018).
[3] H. Kato, *et al.*, J. Phys. Soc. Jpn. **80**, 073701 (2011).
[4] R. Kobayashi, K. Kaneko, and K. Saito, J. Phys. Soc. Jpn. **83**, 104707 (2014).

Charge Redistribution in Dirty Type-II Superconductors Due to Impurity Scatterings in the T-Matrix Approximation.

Muhammad Zafur[1], Hikaru Ueki[2], Takafumi Kita[1]

1. *Department of Physics, Hokkaido University, Sapporo 060-0810, Japan*
2. *Dept. of Mathematics and Physics, Hirosaki University, Hirosaki 036-8560, Japan*

e-mail: zafur@phys.sci.hokudai.ac.jp

In dirty s-wave superconductors, alongside the Lorentz force and the pair-potential gradient (PPG), there exists another source of charge redistribution originally from impurity atom scatterings which are known to affect the magnetic properties of the materials [1][2][3]. In this work, we investigate the charge redistribution of an isolated vortex of s-wave superconductors due to the impurity self-energy in the t-matrix approximation based on the quasiclassical equations for superconductivity [4] and compare its contributions to the charging properties of s-wave superconductors in competition with the Lorentz and PPG forces. Furthermore, we are able to do a numerical comparison between the Born approximation and the more general t-matrix approximation in term of their responses to temperature and Matsubara frequency. The numerical calculations are done by treating the impurity self-energy as a perturbation since its order is very small, hence we can carry out a perturbation expansion of the quasiclassical equations [5]. In contrast with those caused by the Lorentz and PPG forces, we found that the impurity self-energy gives rise to a charge redistribution in which negative charges are accumulated at the vortex center. For the case of medium and strong impurity potential ($\Gamma_n/\Delta_0 \geq 0.5$), the magnitude of charge density due to the impurity self-energy is always slightly larger than the one caused by the Lorentz force and still much smaller than that of the pair-potential gradient. Moreover, maximum charge density in the vortex core is obtained in the Born limit ($\delta_0 = 0$), setting delta to certain value leads to lower charge density. More details regarding results and methods will be presented at the conference.

References

[1] T. Kita, *Statistical Mechanics of Superconductivity* (Springer, Tokyo, 2015).
[2] H. Ueki, W. Kohno, and T. Kita, J. Phys. Soc. Jpn. **85**, 064702 (2016).
[3] M. Ohuchi, H. Ueki, and T. Kita, J. Phys. Soc. Jpn. **86**, 073702 (2017).
[4] T. Kita, Phys. Rev. B **64**, 054503 (2001).
[5] T. Kita, Phys. Rev. B **79**, 024521 (2009).

Dielectric Relaxation Processes in Sugars and Sugar Alcohols

Sho Kubo, Shotaro Kishi, Ryusuke Nozaki
Department of Physics, Hokkaido University, Sapporo 060-0810, Japan,
e-mail: kubo0121@eis.hokudai.ac.jp

Glass forming materials have several types of molecular motions with different time scale. Using dielectric spectroscopy, these motions are observed as relaxation process such as α process, secondary process, boson peak, etc. The origin of α process is considered to be cooperative molecular motions, and secondary process is to be local motions.

Sugars (saccharides) and sugar alcohols, which are typical of energy sources for living things, are glass forming materials. In our group, dielectric measurements of pure sugar, pure sugar alcohols, and mixtures of pure sugar alcohols have been performed. Mixtures of two sugar alcohols have only one α process in spite of the difference in the relaxation time of samples used as mixture, which supports the idea that the origin comes from cooperative motions. On the other hand, the origin of secondary process was poorly understood because it didn't depend on the type of sugar alcohols.

To investigate further the origin of α process and secondary process in sugars and sugar alcohols, we measured dielectric relaxation of mixtures of fructose as sugar and sorbitol as sugar alcohol.

Electronic Superstructures in High-T_c Cuprate $Bi_2Sr_2CaCu_2O_{8+x}$: an STM/STS study

S. Mizuta[1], T. Kurosawa[1], N. Momono[2], H. Yoshida[1], M. Oda[1] and M. Ido[1]

[1]*Department of Physics, Hokkaido University, Sapporo, Japan*
[2]*Department of Applied Sciences, Muroran Institute of Technology, Muroran, Japan*

In the present work, STM/STS measurements were carried out in the superconducting state of underdoped (UD) $Bi_2Sr_2CaCu_2O_{8+x}$ (Bi2212) crystals with a hole doping level of ∼0.12. We investigated the mutual relationship among three types of electronic superstructures such as checkerboard modulation (CBM) [1–4], Cu–O–Cu bond-centered modulation (BCM) [5, 6] and quasiparticle interference modulation (QPIM) [5, 7], by focusing on their spatial dependence.

The STS spectrum measured in the UD samples was well-understood in terms of two energy gaps coexisting in the antinodal region; it exhibits broad peaks corresponding to the pseudogap (PG) at larger energies $|E| = \Delta_{PG}$ and subgap (SG) behavior at smaller energies $|E| = \Delta_{PG}$, which is comparable with the pairing gap size Δ_{pair} (fig. 1(a)). CBM is found in images of the local density of states (LDOS) for energies around Δ_{SG}, whereas BCM is found in those for energies around Δ_{PG} (figs. 1(b) and (c)). These two superstructures, which are characterized by energy-independent wavevectors or nondispersive, are formed in the same regimes within CuO_2 planes. This finding implies that the spatial structure of electronic states in the antinodal region seems to change from CBM to BCM with increasing energy.

Furthermore, we confirmed that CBM coexists with QPIM, which is caused by the interference of Bogoliubov quasiparticles on the nodal Fermi arc hosting the *d*-wave superconducting gap. As is well known, QPIM consists of seven independent components, and each of them is characterized by an energy-dependent wavevector. For one of the components, $\boldsymbol{q}_1$-QPIM, the wavevector is similar to that of the nondispersive CBM at energies around Δ_{SG}, wherein we established a stimulating relation, depending on the polarity of STM bias voltage V_s, between the phases of CBM and $\boldsymbol{q}_1$-QPIM. In this conference, we will report the detailed features on their coexistence.

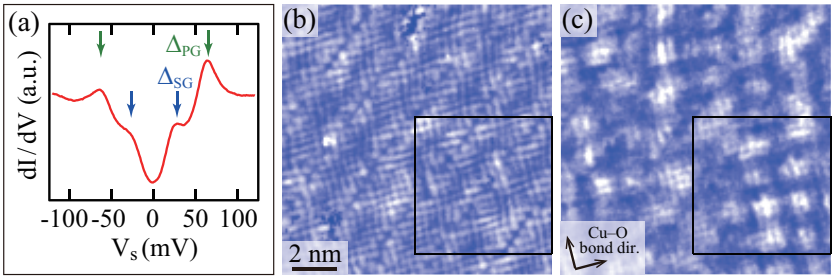

Figure 1: (a) Representative STS spectrum in UD-Bi2212. (b) LDOS images for $V_s = \Delta_{PG}/e$ and (c) for +20 mV ($\sim \Delta_{SG}/e$). BCM and CBM are clearly observed in the boxed region in (b) and (c), respectively.

References

[1]. C. Howald *et al.*, Phys. Rev. B **67**, 014533 (2003).
[2]. R. Comin *et al.*, Annu. Rev. Condens. Matter Phys. **7**, 369 (2016).
[3]. T. Kurosawa *et al.*, J. Phys. Soc. Jpn. **85**, 044709 (2016).
[4]. S. Mizuta*et al.*, J. Phys.: Conf. Ser. **969**, 012071 (2018).
[5]. Y. Kohsaka *et al.*, Nature **454**, 1072 (2008).
[6]. M. H. Hamidian *et al.*, Nat. Phys. **12**, 150 (2016).
[7]. K. Fujita *et al.*, Science **344**, 612 (2014).

Magnetic Properties of Perfect Kagome Lattices in $YCu_3(OH)_6Cl_3$

T. Okada[1] and H. Yoshida[1]

[1]Graduate School of Science, Hokkaido University, Sapporo, Hokkaido 060-0810, Japan

Geometrically frustrated magnets have been investigated due to their nontrivial magnetic state, especially the quantum spin liquid (QSL) state. Herbertsmithite and kapellasite, $ZnCu_3(OH)_6Cl_2$, are the best known S=1/2 quantum kagome (corner-sharing triangular) antiferromagnet and the realization of a QSL state has been proven theoretically. In actual materials, however, their anti-site disordering between magnetic Cu^{2+} and nonmagnetic Zn^{2+} ions in the kagome plane hinders the ground state properties of the kagome compounds.

In order to avoid the anti-site disorder, many efforts have been taken. We have succeessfully synthesized single crystals of the S=1/2 kagome antiferromagnet $CaCu_3(OH)_6Cl_2{\cdot}0.6H_2O$ [1]. This compound was expected for realization of a novel magnetic state with spin fluctuation due to its strong frustration and quantum fluctuation on kagome lattice. Sun *et al.* showed a possible QSL state in $YCu_3(OH)_6Cl_3$ [2]. It crystallizes in the trigonal symmetry with space group P-3m1 and has a perfect kagome lattice without any mixing between magnetic Cu^{2+} and nonmagnetic Y^{3+}. They reported that no magnetic order down to 2 K was observed in magnetic susceptibility.

We have succeeded in preparing single crystals of $YCu_3(OH)_6Cl_3$ as shown in Fig. 1 (c) and have performed the magnetic susceptibility measurements. Figure 2 shows temperature dependences of the magnetic susceptibility on polycrystalline $YCu_3(OH)_6Cl_3$. We found that antiferromagnetic ordering was suppressed below 100 K in this compound.

In my presentation, I will show details of single crystal syntheses and discuss the magnetic properties of perfect kagome antiferromagnet $YCu_3(OH)_6Cl_3$.

This study was supported by the Grant-in-Aid for Scientific Research C (18K03529).

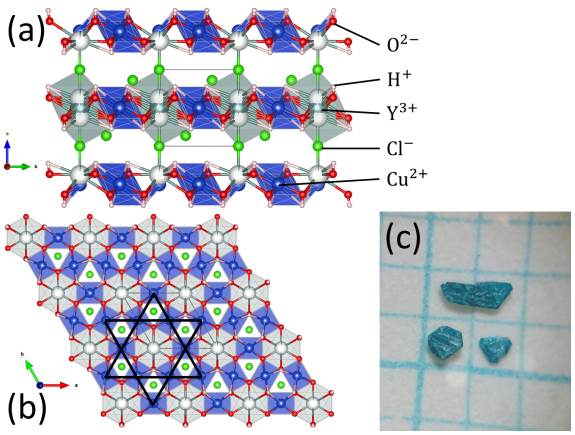

Fig. 1: (a),(b) Crystal structure of $YCu_3(OH)_6Cl_3$ (c) The picture of single crystals obtained in this study.

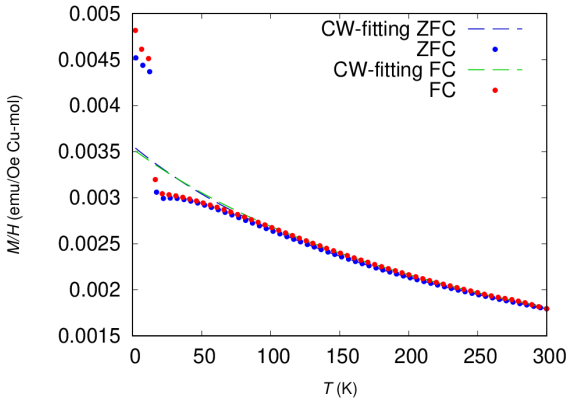

Fig. 2: Temperature dependence of the magnetic susceptibility on polycrystalline sample measured at 1000 Oe.

References

[1] H. Yoshida, *et al.*, Journal of the Physical Society of Japan **86**, 033704 (2017)

[2] W. Sun, Y. X. Huang, S. Nokhrin, Y. M. Pan and J. X. Mi, J. Mater. Chem. C, 2016, **4**, 8772

^{13}C NMR of λ-(BEDT-TTF)$_2$GaCl$_4$ under pressure

Masashi Sawada

Low temperature physics group, Department of Condensed Matter Physics,

Graduate School of Science, Hokkaido University

1. Introduction

Figure 1 shows the universal *P*-*T* phase diagram of λ-(D)$_2$GaCl$_4$ [D = ET (BEDT-TTF), STF, BETS]. λ-(BETS)$_2$GaCl$_4$ salt shows a SC transition at 5 K. Previous ^{13}C NMR study has revealed that an AF spin fluctuation exists before the SC transition [1]. Hence, it has been expected that the SC transition is driven by AF spin fluctuation. However, the adjacent phase to the SC phase is a nonmagnetic insulating phase. Although λ-(ET)$_2$GaCl$_4$ shows an AF ordering below 13 K at ambient pressure [2], λ-(STF)$_2$GaCl$_4$ does not show AF ordering down to lowest temperature. In general, STF molecule has an asymmetric arrangement of S and Se atoms. Hence, it is possible that the asymmetry of STF molecule plays as a role of disorder and prevents an AF ordering in STF salt [2]. To reveal the nature of the magnetic property of λ-(D)$_2$GaCl$_4$ in the intermediate pressure region, we have performed ^{13}C NMR under pressure for λ-(ET)$_2$GaCl$_4$ which does not have an asymmetry in the donor molecule.

2. Experiments

Single crystals of λ-(ET)$_2$GaCl$_4$ were synthesized by electrochemical method. ^{13}C NMR was performed under magnetic field of 6 T and under pressure 2.5 kbar. The NiCrAl alloy clamp cell and Daphne 7474 oil were used for pressurizing. We have measured the spin-lattice relaxation time (T_1) for 2-100 K.

3. Results and Discussion

Figure 2 shows the temperature dependence of the $1/T_1T$. Below 25 K, $1/T_1T$ rapidly increases with decreasing temperature and has a peak at 3 K. This behavior indicates the AF transition occurs at 3 K and

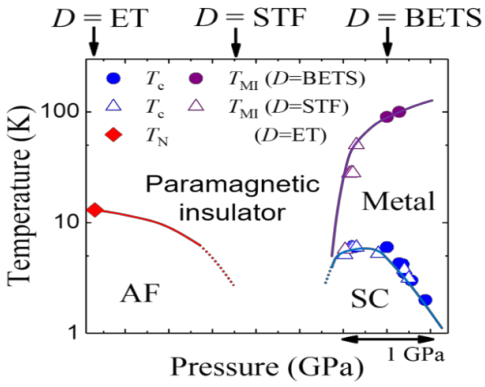

Fig. 1 The universal *P*-*T* phase diagram of λ-(D)$_2$GaCl$_4$

AF phase is suppressed by applying pressure. This implies that nonmagnetic phase of STF salt is not due to the asymmetry of STF molecule, instead, it is an intrinsic property.

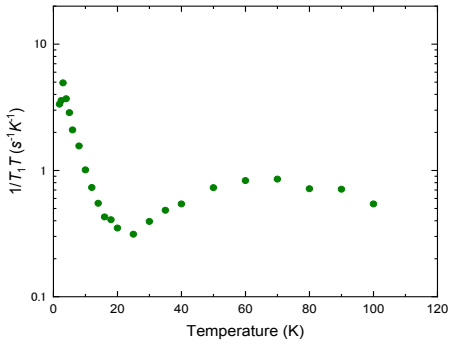

Fig. 2 The temperature dependence of $1/T_1T$

4. Conclusion

We have performed ^{13}C NMR for λ-(ET)$_2$GaCl$_4$ under pressure 2.5 kbar and confirmed that the temperature dependence of $1/T_1T$ has a peak at 3 K.

References

[1] T. Kobayashi, doctor thesis (2018).

[2] Y. Saito *et al*. JPSJ **87**, 013707 (2018).

Motivation for supersymmetry theory

Department of Physics, Hokkaido University

Yuta Mimura

Standard Model is verified by many experiments but has several unsolved problems. Hierarchy problem is one of that. By introducing Supersymmetry we can solve it and also can get some by-products such as giving a candidate for Dark Matter. In this session, I explain mainly Hierarchy problem and how supersymmetry theory solves it, then refer to other beneficial predictions that are given by considering Supersymmetry.

Domain Wall

Seiya Yamada

Department of Physics, Hokkaido University

Abstract

In the early universe, the universe whose vacuum was considered to have high symmetry had high density and high temperature. The temperature of the universe fell down due to the expansion of space. Then, it is considered that phase transition had occured due to the spontaneous symmetry breaking (SSB) and produced topological defects.

I am going to introduce a domain wall which is an example of a topological defect associated with SSB by using a simple scalar model. Consider a Lagrangian of a real scalar field

$$\mathcal{L} = \frac{1}{2}\left(\partial_\mu \phi\right)^2 - \frac{1}{4}\lambda\left(\phi^2 - \sigma^2\right)^2 .$$

The symmetry of the Lagrangian is spotaneously broken when scalar field ϕ takes two vacuum expectation values (VEV). Then, space is divided into two regions ($\phi = +\sigma$, $\phi = -\sigma$). A Domain wall that has energy occurs at the boundary between the two regions.

We can estimate the surface energy density associated with the domain wall. I will show the value of energy in this poster session.

Next, I will briefly explain Cosmic string which is one dimensional topological defect. Since Cosmic string is closely related to cosmology, cosmic string have been studied intensively.

References

[1] Kolb, Edward W. and Turner, Michael S, "The Early Universe"

Peculiar Magnetization Reversal of $TbNiC_2$

M. Yamamoto[1], H. Hidaka[1], T. Yanagisawa[1], C. Tabata[2], H. Nakao[2], S. Shimomura[3], H. Onodera[4], and H. Amitsuka[1]

[1]*Dept. of Physics, Hokkaido Univ., Sapporo 060-0810, Japan*
[2]*Condensed Matter Research Center and Photon Factory, Institute of Materials Structure Science, High Energy Accelerator Research Organization, Tsukuba 305-0801, Japan*
[3]*Dept. of Physics, Kyoto Sangyo Univ., Kyoto 603-8555, Japan*
[4]*Dept. of Physics, Graduate School of Science, Tohoku Univ., Sendai 980-8578, Japan*

$TbNiC_2$ has attracted much attention because of its rich and interesting properties of spin and charge ordering. It crystallizes in a noncentrosymmetric *A*-centered orthorhombic $CeNiC_2$-type structure with a space group *Amm*2 (C_{2v}^{14}, No. 38) [1]. The system exhibits a charge density wave (CDW) order with an incommensurate propagation vector $\boldsymbol{q}_1$ of (0.5, η, 0) at 243 K and two successive commensurate ones with $\boldsymbol{q}_{1C}$ of (0.5, 0.5, 0) and $\boldsymbol{q}_2$ of (0.5, 0.5, 0.5) at 160 K and 128 K, respectively. The commensurate CDW ordering state with $\boldsymbol{q}_{1C}$ persists even when the system undergoes an antiferromagnetic (AFM) transition at $T_N = 25$ K [2]. The reported magnetic structure is a noncollinear type described by the same propagation vector as $\boldsymbol{q}_{1C}$ with the Tb moments of 6.8 μ_B, where Tb moments are canted by about 13° from the *c* axis and by about 7° from the *b* axis [3,4]. The above-mentioned multiple phase transitions in $TbNiC_2$ imply an intriguing interplay between CDW and AFM [2]. Moreover, the system exhibits a weak spontaneous magnetization *M* of about 0.22 μ_B in the AFM state [5]. Although the above-mentioned magnetic structure cannot explain this weak ferromagnetic component, there are few studies in low-magnetic fields thus far. We thus focus on the magnetic response to low-magnetic fields in order to reveal the origin of the weak ferromagnetism of this system.

In the present study, the magnetization for the single-crystalline samples of $TbNiC_2$ along different field directions were measured in the temperature range from 2 to 300 K with applied magnetic field up to 15 kOe. Figure 1 shows *M* as a function of temperature upon field cooling (FC) in various magnetic fields along the *c* axis. We found that *M* in the FC process decreases below T_N across zero with decreasing temperature, and becomes negative with fields lower than 500 Oe. It is revealed that this unusual "magnetization reversal" occurs only below T_N and only in the FC process. As can be seen in Fig. 2, it is clear that the observed magnetization reversal is not due to a conventional diamagnetism such as the core diamagnetism or Landau diamagnetism since the differential susceptibility is always positive. We will discuss the origin of this peculiar magnetization reversal of $TbNiC_2$.

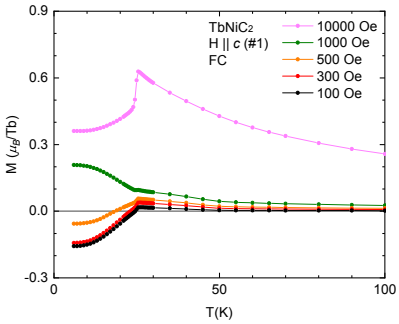

Fig. 1. Temperature dependences of the magnetization upon FC in various magnetic fields along the *c* axis.

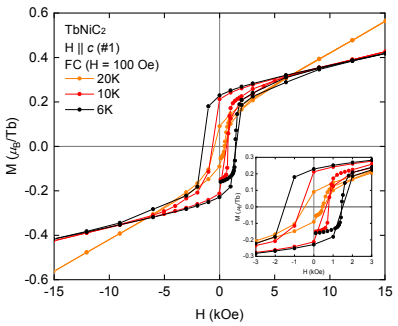

Fig. 2. Isothermal magnetization processes measured at several temperatures for magnetic field along the *c* axis after FC at 100 Oe.

References

[1] W. Jeitschko *et al*., J. Less-Common Met. **116**, 147 (1986).
[2] S. Shimomura *et al*., Phys. Rev. B **93**, 165108 (2016).
[3] J.K. Yakinthos *et al*., J. Magn. Magn. Mater. **81**, 163 (1989).
[4] N. Uchida *et al*., J. Magn. Magn. Mater. **145**, L16 (1995).
[5] H. Onodera *et al*., J. Magn. Magn. Mater. **137**, 35 (1994).

Electrical Properties of λ'-(BEDT-STF)$_2$GaBr$_4$ at High Pressures

Satoshi Kawaguchi, Takuma Wada, Takaaki Minamidate, Masashi Sawada, Noriaki Matsunaga, Atsushi Kawamoto, Kazushige Nomura
Department of Physics, Hokkaido University, Sapporo 060-0810, Japan
Email: kawaguchi-satoshi@eis.hokudai.ac.jp

A quasi-two-dimensional organic conductor λ-(BETS)$_2$GaCl$_4$ shows superconducting phase at 5.5 K at ambient pressure.[1] Recently, we found that λ-(BEDT-STF)$_2$ GaCl$_4$ locates at lower pressure region than that of λ-(BETS)$_2$GaCl$_4$ and the phase adjacent to the SC phase in λ-type systems is not the antifferro magnetic phase.[2] In contrast, λ'-(BETS)$_2$GaBr$_4$ shows the transition from a (semi)metallic state to the insulating state at 50 K.[3] To clarify the origin of MI transition and the difference from the λ-type salt, we performed the resistivity measurements under pressure, magnetic susceptibility measurements at ambient pressure and NMR measurements.

Single crystals of new material λ'-(BEDT-STF)$_2$GaBr$_4$ were synthesized by the standard electrochemical method. Gold wires were attached to the crystal with carbon paste as electrodes. The crystal was mounted inside a BeCu and NiCrAl hybrid cramp cell with Daphne 7373 oil as a pressure medium. We measured the resistivity under pressure and the magnetic susceptibilities at ambient pressure of λ'-(BEDT-STF)$_2$GaBr$_4$. λ'-(BEDT-STF)$_2$GaBr$_4$ shows insulating state in whole temperature region. This insulating behavior was gradually suppressed with increasing pressure. The transition temperature decrease with increasing pressure. This transition is thought to be correspond to the transition to the insulator phase which observed in λ'-(BETS)$_2$GaBr$_4$ around 50 K at ambient pressure. We concluded that λ'-(BEDT-STF)$_2$GaBr$_4$ locates at the lower pressure region than that of λ'-(BETS)$_2$GaBr$_4$ in the universal phase diagram and the insulator phase appears in the wide pressure region. The magnetic susceptibility at ambient pressure decreased rapidly below 50 K. Subtracting the Curie component, the core diamagnetism and the contribution of stycast, the magnetic susceptibility approached to zero. So λ'-(BEDT-STF)$_2$GaBr$_4$ is thought to show the transition to non-magnetic state. NMR spectra of the λ'-(BEDT-STF)$_2$GaBr$_4$ at ambient pressure does not show temperature dependence. The spin-lattice relaxation rate $1/T_1$ drastically decreases at 50K and slowly decreases below 50 K. The decrease of $1/T_1$ is consistent with the transition of magnetic susceptibility. However this non-magnetic state is not simple spin-Peierls state because $1/T_1$ gradually decreases below 50 K.

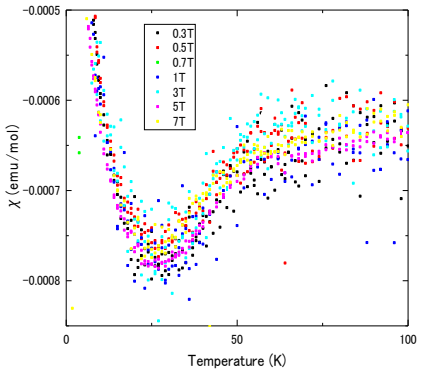

Fig. 1. Magnetic susceptibility at ambient pressure of λ'-(BEDT-STF)$_2$GaBr$_4$

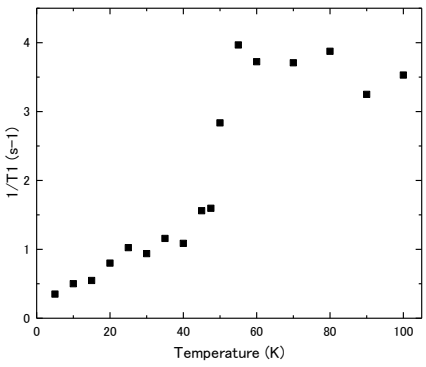

Fig. 2. $1/T_1$ at ambient pressure of λ'-(BEDT-STF)$_2$GaBr$_4$

References

[1] H. Kobayashi, *et al, Chem. Lett.*, **22**, 1559 (1993)
[2] T. Minamidate, *et al, JPSJ*, **84**, 063704 (2015)
[3] H.Tanaka, *et al, Chem. Lett*., **28**, 133, (1999)

Electronic Properties in SDW Phase of Quasi-One-Dimensional Organic Conductor (DMET-TTF)$_2$AuBr$_2$

Yoshiaki Sasaki, Tomoaki Tsuchiya, Noriaki Matsunaga, Atsushi Kawamoto, and Kazushige Nomura
Department of Physics, Hokkaido University
Email: ysasaki_epldc@eis.hokudai.ac.jp

The DMET-TTF, where DMET-TTF dimethyl(ethylenedithio)tetrathiafulvalen, molecular is a hybrid structure between TMTTF and BEDT-TTF. In a similar substance (DMET)$_2X$ (X is a linear monovalent anion), where DMET is dimethyl(ethylenedithio)diselenadithiofuluvalen, donor molecules stack to form columns along the b-axis, and this salt has a quasi-one-dimensional Fermi surface[1]. For example, (DMET)$_2$Au(Cn)$_2$ undergoes metal-SDW transition around 20 K at ambient pressure and superconducting transition at 0.15 GPa[1]. (DMET-TTF)$_2$AuBr$_2$ determined by X-ray diffraction is isostructural compound with (DMET)$_2X$ (X is $CuCl_2$[1] and Au(CN)$_2$[2]), so this salt has quasi-one-dimensional Fermi surface.

We have investigated pressure dependence of electric properties of (DMET-TTF)$_2$AuBr$_2$. Figure 1 shows the temperature dependence of resistance and figure 2 shows the phase diagram of (DMET-TTF)$_2$AuBr$_2$. At 0.3GPa, metallic state was observed at high temperature, and metal-insulator transition was observed at 38.8 K and 16.8 K for 0.3 GPa and 0.6 GPa, respectively. The M-I transition temperature decreases with increasing pressure. The superconducting transition was also observed at 3.38 K under 0.85 GPa. The resistance was well described by thermally activation type in insulator phase. From the analogy with phase diagram of (DMET)$_2$Au(CN)$_2$[3], the M-I transition has been considered SDW transition. In SDW phase, the definite threshold electric field and increase of SDW transition temperature T_{SDW} with increasing magnetic field were observed. In particular, we have focused on the SDW sliding, and performed non-linear conduction measurements at various temperature.

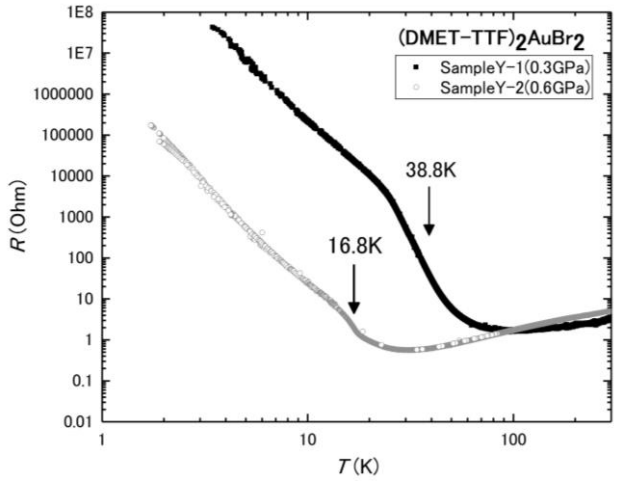

Fig. 1. The temperature dependence of resistance under 0.3GPa and 0.6GPa.

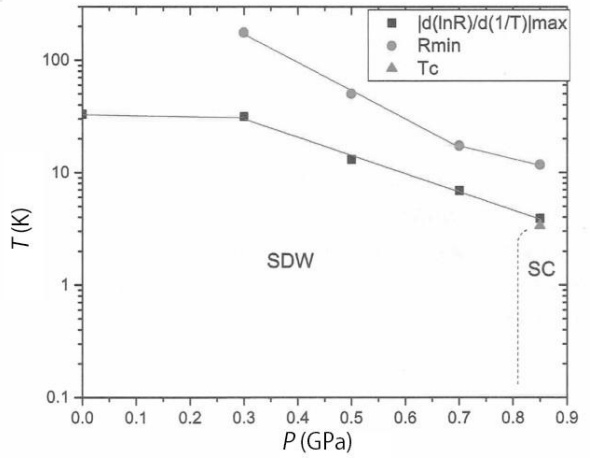

Fig. 2. The phase diagram of (DMET-TTF)$_2$AuBr$_2$.

References

[1]H. Ito *et al*., *PRB*, **71**, 212503 (2005)
[2]K. Kanoda *et al*., *PRB*, **38**,39 (1988).
[3]H. Yoshino *et al*., *JPSJ*, **64**, 2307 (1995)

Ultrasonic Study of Quadrupolar Response in CeTe under Hydrostatic Pressure

T. SAITO[1], H. MATSUMORI[1], H. HIDAKA[1], T. YANAGISAWA[1], H. AMITSUKA[1], Y. HAYASHI[2], T. MATSUMURA[2], S. NAKAMURA[3] and A. OCHIAI[4]

[1]*Graduate School of Science, Hokkaido University, Sapporo 060-0810, Japan* [2]
[2]*Department of Quantum Matter, AdSM, Hiroshima University, Higashi-hiroshima, Hiroshima 739-8530, Japan*
[3]*Institute for Materials Reserchment, Tohoku University, Sendai 980-8577, Japan*
[4]*Department of Physics, Graduate School of Science, Tohoku University, Sendai 980-8578, Japan*

A Kondo compound CeTe has NaCl-type cubic structure ($Fm\bar{3}m$, O_h^5, No. 225), where the CEF (crystalline electrical field) ground state of $J = 5/2$ multiplet splits into Γ_7 doublet and Γ_8 quartet. This material has previously been considered as a simple antiferromagnet [1]. Recent studies of electrical resistivity, Magnetization and specific heat under hydrostatic pressure, however, reveal that the CEF levels of these systems are getting degenerated by applying pressure and antiferroquadrupolar (AFQ) phase will be appeared under applied magnetic fields or applying pressure above 1 GPa [2]. In the present study, we investigated elastic constant C_{44} of CeTe by means of ultrasound under hydrostatic pressure $P < 2.45$ GPa. For the hydrostatic pressure measurements, a new technique has been developed and used for the present experiments, which has allowed high-frequency ultrasonic measurements under pressure by installing a pair of ultra-thin semi-rigid coaxial cables with a diameter of 0.33 mm into a hybrid piston-cylinder cell. [3] Figure 1(a) shows temperature dependences of the elastic constant C_{44} of CeTe at P = 2.45 GPa. The C_{44} decreases with decreasing temperature and shows several anomalies below about 6 K. Figure 1(b) shows the magnetic field dependences of the elastic constant C_{44} of CeTe. Figure 1(c) shows the temperature-magnetic field phase diagram of CeTe defined by anomalies of temperature dependence and magnetic field dependence. Phase IV is assumed AFQ phase by resent study [2]. I-IV phase line consistent with resent phase diagram by magnetization and specific heat. Phase V and dot lines are found newly by elastic constants. Based on investigation of the hydrostatic pressure variation of the elastic constant, we can obtain additional information regarding the hybridization between conduction electron and *f*-electron, *c-f* hybridization, and its consequences on the modification of the CEF level scheme change under pressure.

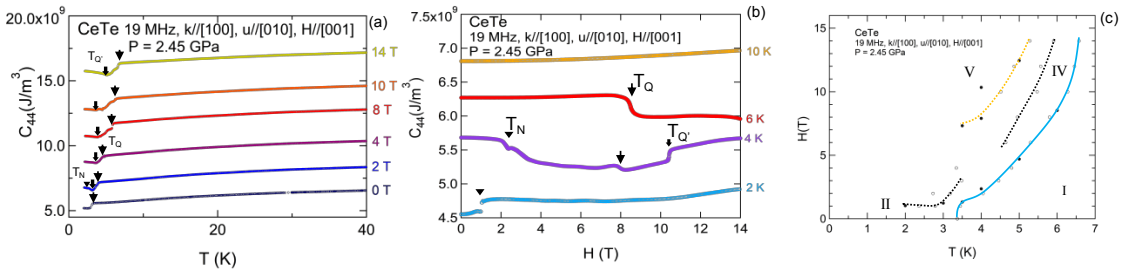

Fig. 1: Temperature Dependence(a) and Magnetic Field Dependence(b) of Elastic Constant C_{44} of CeTe at P = 2.45 GPa and Temperature-Magnetic Field Phase Diagram(c)

[1] H. Matsui, T. Goto, A. Tamaki, T. Fujimura, T. Suzuki, and T. Kasuya, J. Mag. Mag. Mat. **76&77** (1988) 321.
[2] H. Takaguchi, Y. Hayashi, T. Matsumura, K. Umeo, M. Sera, and A. Ochiai, J. Phys. Soc. Jpn. **84** (2015) 044708.
[3] S. Mombetsu, T. Murazumi, H. Hidaka, T. Yanagisawa, H. Amitsuka, P.-C. Ho, and M. B. Maple, Phys. Rev. B **94** (2016) 085142.

Superconductivity in Cu-doped $TaSe_3$: Relationship between superconductivity and induced charge density wave

Atsushi Nomura,[1] Kazuhiko Yamaya,[2] Shigeru Takayanagi,[2] Koich Ichimura,[1,2] and Satoshi Tanda[1,2]

[1] Department of Applied Physics, Hokkaido University

[2] Center of Education and Research for Topological Science and Technology, Hokkaido University

The relationship between superconductivity (SC) and charge density wave (CDW) has been a major research topic in condensed matter physics and has been investigated in many materials. However, previous studies were actually limited to two cases: the first is where SC and a CDW intrinsically coexist in a material; the second is where SC is induced in a CDW material. Here, in addition to these two cases, we should also investigate the relationship in a third case where a CDW is induced in a superconducting material, if we are to gain a universal understanding.

Recently, we reported that the CDW transition is induced by Cu doping in $TaSe_3$ which is a superconducting material [1]. Therefore, in this study, we investigated SC in Cu-doped $TaSe_3$ by measuring the temperature dependence of the resistance to clarify the effect of Cu doping on SC and the relationship between SC and an induced CDW.

We observed an emergence of a region where the SC transition temperature decreases in samples with higher Cu concentrations and found that the region tended to expand with increasing Cu concentration. In addition, the temperature dependence of the upper critical field of Cu-doped $TaSe_3$ was found to differ from that of pure $TaSe_3$. Based on these experimental results and the fact that the SC of $TaSe_3$ is filamentary, we conclude that SC is suppressed locally by Cu doping and competes with the CDW in Cu-doped $TaSe_3$. The resistance anomaly due to the CDW transition was extremely small and the size of the anomaly was enhanced with increasing Cu concentration but the temperature at which the anomaly appeared hardly changed. This result of the anomaly and the local suppression of SC imply that the induced CDWs are short-range order in the vicinity of Cu atoms.

[1] A. Nomura, K. Yamaya, S. Takayanagi, K. Ichimura, T. Matsuura, and S. Tanda, EPL 119, 17005 (2017).

Various physical properties of VO_2 film by controlling deposition temperature

Yesul Choi[1,3], Dooyong Lee[1,3], Ji Woong Kim[1], Sehwan Song[1], Jong-Seong Bae[2], Jaekwang Lee[1] and Sungkyun Park[1,*]

[1]*Department of Physics, Pusan National University, Busan 46241, Korea*
[2]*Busan Center, Korea Basic Science Institute, Busan 46742, Korea*
[3]*Advanced Nano Surface Research Group, Korea Basic Science Institute, Daejeon 34133, Korea*

Abstract

Vanadium dioxide (VO_2) shows an insulator-metal transition (IMT) at 68 ^oC. There are several explanations of the IMT mechanism, such as the Peierls transition (i.e., structural transition), the Mott transition (i.e., electronic transition) or collaborative Mott-Peierls transition. In this study, VO_2 films grown on Al_2O_3(001) substrate were deposited at various temperatures (e.g., 500 ^oC ~ 720 ^oC) to examine the correlation effect between the vanadium multivalent (V^{3+}, V^{4+}, V^{5+}) and structural properties, and IMT characteristics systematically. As a result, the IMT temperature and the resistivity ratio (ρ(26 ^oC)/ ρ(100 ^oC)) are the greatest for the films deposited at 600 ^oC and 650 ^oC owing to the change of V^{5+} to V^{4+} and the out-of-plane strain relaxation. On the other hand, for the films deposited above 650 ^oC, the transition temperature and resistivity ratio sharply decreased owing to the increase in V^{3+} state (i.e., additional electrons), which reduced the thermal energy barrier for IMT. These results provide the experimental evidence for a specific mechanism for IMT transition in separately.

This study was supported in part by NRF Korea (NRF-2015R1D1A1A01058672 and NRF-2018R1D1A1B07045663).

* Correspondence should be addressed to Sungkyun Park (psk@pusan.ac.kr)

Thickness Dependent Magnetic Properties of FeRh/MgO films

Sehwan Song, Jiwoong Kim, Dooyong Lee, Sungkyun Park*
Department of Physics, Pusan National University, Korea

FeRh shows meta-magnetic first-order phase transition above 350 K accompanied with isotropic lattice expansion and variation of the magnetoresistance. These are great interests for future applications such as, heat assisted magnetic random access memories (HAMRAM), magnetic cooling and spintronic devices [1, 2]. In particular, film form of FeRh showed modified magnetic properties owing to the presence of interface (bottom and/or top). For example, the formation of ferromagnetic (FM) domain nucleation at the interface owing to the interfacial strain and chemical diffusion of Fe or Rh can easily modify the antiferromagnetic (AFM) characteristics below transition temperature of the films [3, 4]. Therefore, it is important to understand the role of interface of films and gain the physical insights.

In this study, we investigated the structural, chemical and magnetic properties FeRh/MgO(100) films by varying deposition time (1, 2, 5, 10 min). Interestingly, the phase transition temperature increased and magnetization at AFM region decreased as deposition time increased. The detailed structural and chemical analysis were performed to obtain possible correlation between local structural ordering and physical property variations.

[1] S. Yuasa et al., J. Appl. Phys. **83**, 6813 (1998).
[2] Y. Liu et al., Nat. Commun. **7**, 11614 (2016).
[3] C. Gatel et al., Nat. Commun. 8, 15703 (2017).
[4] R. Fan et al., Phys. Rev. B **82**, 184418 (2010).

This research is supported in part by NRF Korea (NRF-2015R1D1A1A01058672 and NRF-2017K1A3A7A09016305).

*E-mail: psk@pusan.ac.kr

Finite Size Effects in La_2CuO_4 Nanoparticles Probed by μSR and NMR

S. Winarsih[1,2], F. Budiman[3], H. Tanaka[3], T. Goto[4], T. Adachi[4], B. Kurniawan[2], I. Watanabe[1,2]

[1]*Meson Science Laboratory, RIKEN, Wako 351-0198, Japan*
[2]*Department of Physics, Universitas Indonesia, Depok 16424, Indonesia*
[3]*Department of Human Intelligence Systems, Kyushu Institute of Technology, Kitakyushu 808-0196, Japan*
[4]*Department of Engineering and Applied Sciences, Sophia University, Tokyo 102-8554, Japan*

Finite size effects, which refer to the reduction in particle size until they become nanoscale sized, will introduce novel phenomena in magnetic materials [1-3]. For instance, Zheng *et al*. reported that by reducing CuO particles down to ~5 nm, the Néel temperature, T_N, was drastically decreased to 30 K, compared with bulk CuO which has T_N=229 K [3]. We examined such kind of nano-sized effects in the typical Mott insulator La_2CuO_4 (LCO) by using muon spin relaxation (μSR) and NMR methods. Fig. 1 shows that muon spin precession started to be observed around 35 K in LCO with particle size of 69 nm. It means long-range magnetic ordering appear at much lower temperature than that observed in bulk LCO (~300 K). However, muon spin precession in nanoparticle case was strongly damped compared with bulk one. The saturated internal field at the muon sites was determined to be about 420 G. This value was almost the same as that observed in bulk LCO. It is implied that the average magnetic moment of bulk LCO and nano-LCO are same but magnetic interaction might be changed due to nano-sized effect. The ^{139}La-NMR results also show that internal field has started to appear around the same temperature as that estimated from μSR under zero-field (ZF) condition. μSR and NMR results of LCO nanoparticles and possible reasons of the reduction in T_N in nano-sized LCO will be presented.

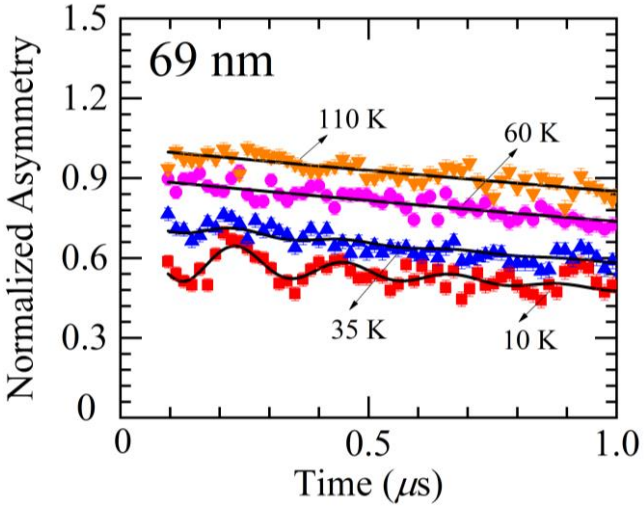

Fig. 1: ZF-μSR of La_2CuO_4 with a particle size of 69 nm measured at various temperatures. Solid lines are the best-fit results assuming the single cosine function to reproduce the muon-spin precession behavior.

References

[1] A. Punnoose *et al*., Phys. Rev. B **64**, 174420 (2001).
[2] Y. J. Tang *et al*., Phys. Rev. B **67**, 054408 (2003).
[3] X. G. Zheng *et al*., Phys. Rev. B **72**, 014464 (2005).

TBA

μSR Studies on Electron Motion Along DNA Molecule

*H. Rozak[1,2)], W.N. Zaharim[2)], S.N. Abu Bakar[2)], N.Ismail[2)],F. Astuti[1,3)], M.I. Mohamed-Ibrahim [2)] ,S. Sulaiman[2)] and I. Watanabe[1,2,3)].

[1)] RIKEN Nishina Center, [2)] Universiti Sains Malaysia ,[3)] Hokkaido University

Deoxyribonucleic acid (DNA) is known as biological molecule that containing the genetic code for all living species. The structure of DNA is consisting of four nitrogenous bases; adenine(A), guanine(G), cytosine(C) and thymine(T) attached to a sugar and phosphate group and arranged in base-pairs in a double helix structure. One of the unique feature of DNA is the π-π interactions of the stacked base-pairs which could lead to the conducting behavior of electron transport. Electron transport studies in DNA is important not only for understanding the DNA damage and repair mechanisms, but also for possible applications as bio-devices. From previous studies, two mechanisms of electron transport have been proposed, namely the tunneling and hopping mechanisms [1]. In order to study the electron transport phenomena, we have carried out μSR measurement on the 12-mer single strands (A, G, C and T) molecule at 100 K and 300 K. Figure 1 (a) shows μSR time spectra from one of those models which is a 12-mer adenine at 300K, with longitudinal magnetic fields up to 4000 G. As can be seen in Figure 1, the muon-spin relaxation behavior is faster at ZF and at higher LF the relaxation behavior however not completely suppressed. This indicates that the muon feels strongly fluctuating internal fields. This is clearly shows that electrons are moving along the single strand molecule and as well as generating fluctuating internal fields that influence the muon. Figure 1(b) shows the applied field dependence of the muon-spin relaxation rate. This behaviour of the graph reflects the dimensionality of the electron motion. From the previous studies 1 D diffusion behavior observed the relaxation rate $\propto LF^{-0.5}$ [2], the result of our experiment however does not show clear 1 D diffusion because λ(B) is not approximated to be proportional $B^{-0.5}$. This might be due to geometrical structure of the the single strand DNA molecule that does not form an ideal 1 D structure. Currently scanning tunnelling microscope measurement being performed to determine the molecular structure of DNA samples.

a)

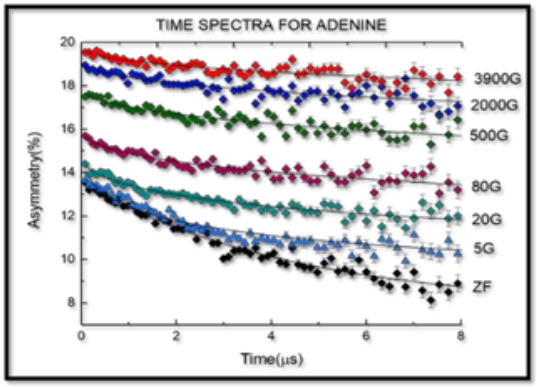

b)

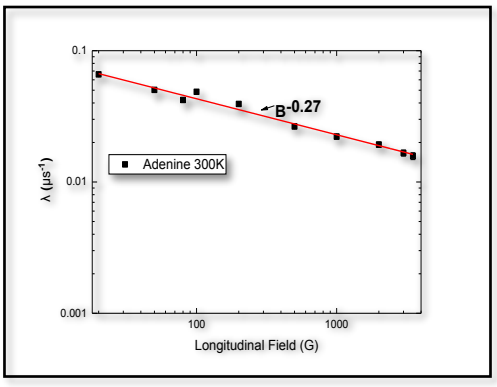

Figure 1. (a) μSR time spectra of the single strand DNA adenine. (b) The applied magnetic-field dependence of the muon-spin relaxation rate for 12-mer adenine measured at 300 K.

References

1. Boon, E. M., & Barton, J. K. (2002). Charge transport in DNA. Current opinion in structural biology, 12(3), 320-329.
2. Butler, M. A., Walker, L. R., & Soos, Z. G. (1976). Dimensionality of spin fluctuations in highly anisotropic TCNQ salts. The Journal of Chemical Physics, 64(9), 3592-3601.